The Pennsylvania State University

The Graduate School

PREVENTING THE FORMATION AND AGGLOMERATION OF CLATHRATE HYDRATES

A Thesis in

Chemistry

by

Gary Love

Submitted in Partial Fulfillment

of the Requirements

for the Degree of

Master of Science

August 2021

The thesis of Gary Love was reviewed and approved by the following:

Lauren Zarzar
Assistant Professor of Chemistry
Thesis Advisor

Ayusman Sen
Verne M. Willaman Professor of Chemistry
Distinguished Professor of Chemistry
Professor of Chemical Engineering

Miriam Freedman
Associate Professor of Chemistry
Associate Department Head for Climate and Diversity

Ralph Colby
Professor of Materials Science and Engineering and Chemical Engineering

Phil Bevilacqua
Distinguished Professor of Chemistry
Distinguished Professor of Biochemistry and Molecular Biology
Department Head, Chemistry

Abstract

Clathrate hydrates have been a continual issue in deep-water pipelines. Since oil remains the most used source of energy, it is important to ensure the pipelines work effectively. There are many known hydrate inhibitors in existence, but each have their own drawbacks or limitations. Our aim is to combine two hydrate inhibitors in order to create an inhibitor with the properties of both that would be able to mitigate the other inhibitors weaknesses. Solid particles were combined with a known hydrate inhibitor in order to analyze the effectiveness of the combination. It was found through optical microscopy that the hydrate formation was random for most systems despite the change in variables. There was no trend found to describe the effectiveness of the new inhibitor, but there was a noticeable impedance on hydrate formation using the inhibitor. More work and studies will need to be done before complete conclusions can be made on the overall effectiveness of the inhibitor, however early results show a promising future for inhibitors like these.

Table of Contents

Abbreviations

CP = cyclopentane

Vinyl silane = vinyltriethoxy silane

Hexadecyl silane = trimethoxyhexadecyl silane

Octyl silane = octyltriethjoxy Silane

o/w = oil-water

MEG = monoethylene glycol

THI = thermodynamic hydrate inhibitor

KHI = kinetic hydrate inhibitor

AA = anti-agglomeration agent

LDHI = low dosage hydrate inhibitor

PVP = polyvinyl pyrrolidone

PVCap = polyvinyl caprolactam

Poly(VP/VC) = polyvinyl pyrrolidone caprolactam

List of Figures

Chapter 1: Introduction

Clathrate Hydrates

Clathrate hydrates are an ice-like substance with a host-guest interaction between water and a smaller hydrophobic guest. They have been studied for various reasons, including pipeline blockages[1], cold storage technology[2], and environmental concerns.[3] There are multiple structures of gas hydrates, dependent on the guest molecule and, in the case of multiple gases, the gas composition.[4] Water molecules form a cage bound together by hydrogen bonds, surrounding a hydrophobic guest molecule and then freeze to form the hydrate structures (figure 1).[5,6] These structures are not classified as ice since it can form at temperatures higher than the freezing point of water and also requires the existence of a small hydrophobic guest.

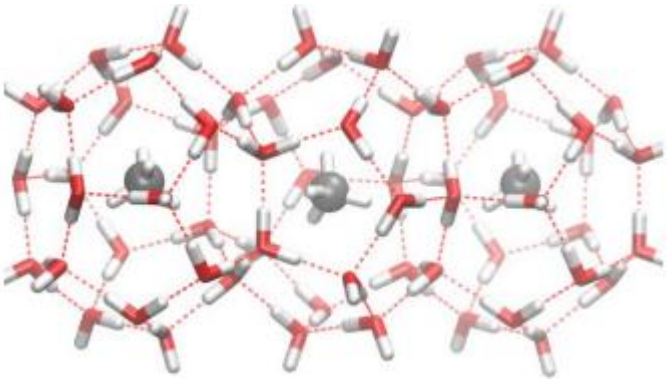

Figure 1. Structure of a methane hydrate. The water molecules form a cage surrounding the hydrophobic methane molecules.[7] The system would collapse or fail to form without the presence of the small hydrophobic guest molecule.

The guest molecules help stabilize the cage-like structure surrounding it.[8] The hydrophobic molecule assembles the water molecules into an adjustable cluster that ultimately becomes the cage-like structure.[9]

The kinetics of the formation of the hydrates also differs from that of the

formation of ice. Hydrates form in high pressure, low temperature environments where the hydrophobic guest molecule meets with water, meaning deep sea conditions are incredibly conducive to clathrate hydrate formation.[10] Methane can be deposited into deep bodies of water through runoffs, seeps, vents, and underwater volcanoes.[11] These variables all allow for methane hydrates to commonly form in deep water environments.

Motivation

Society is heavily reliant on the modern advancements in technology that makes life more comfortable and efficient. The increase in advancement comes with a larger need for energy to power these technologies.[12] Renewable and alternative energy sources have been on the rise globally over the last few decades; however, they are not yet capable of meeting the increasing demand for energy. Oil remains the largest source of energy globally.[13] Since crude oil is not readily available in many places, transporting it usually must be done over long distances to meet growing energy demands. A common mode of transport that is used are oil pipelines, which in many cases lie at the bottom of bodies of water.[14] As mentioned before, these environments can be conducive to hydrate formation due to the high pressure and low temperature conditions.

Clathrate hydrates can be problematic for pipelines, as they can agglomerate to cause blockages which disrupt the flow of the oil.[5,6] Oil pipelines contain a complex mixture of oil, gas, and water, as well as other solid particulates.[15] The oil and water create an emulsion, which exists when two immiscible liquids are mixed. Since there is a larger volume of oil than water in a pipeline, the water breaks up into droplets

dispersed throughout the oil, stabilized by natural surfactants and particulates that are flowing in the pipeline. Some of the emulsion stabilizers are resins, asphaltenes, waxes, clays, mineral scales, and corrosion products that flow in the crude oil system.[16] Clathrate hydrates form where the water, oil, and gas meet.[17] As the hydrates continue to form, they also begin to agglomerate, causing blockages in the pipelines (figure 2). Preventing hydrate formation and fixing plugging in pipelines can cost millions of dollars, meaning it is important to continue improvement on methods of inhibition.[18] The goal of this work is to utilize particles at the interface to stabilize the emulsions and ultimately act as barriers for the agglomeration of the hydrates.

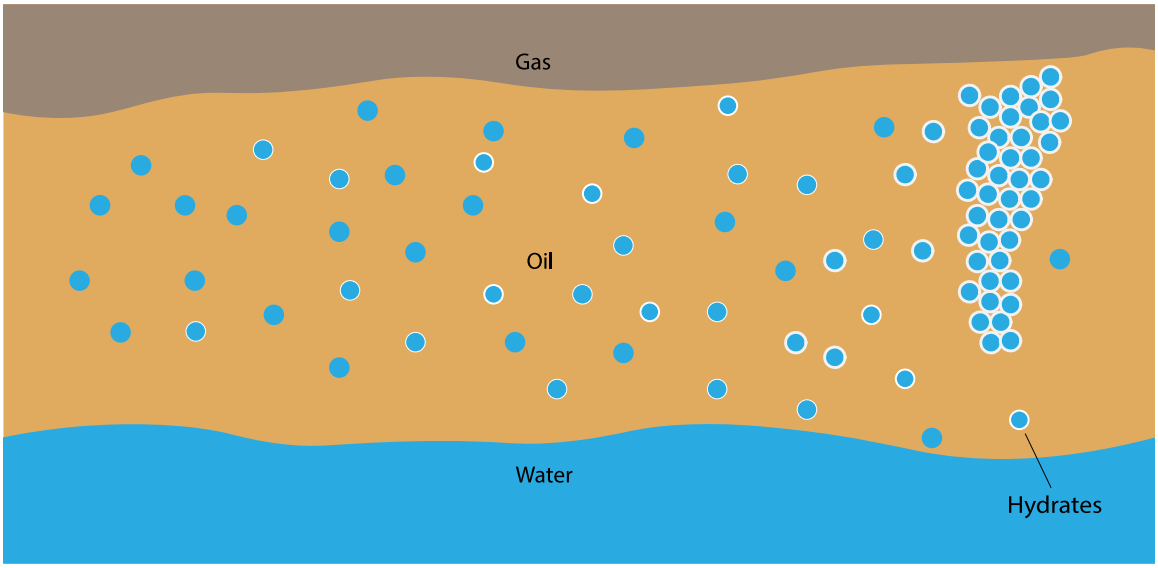

Figure 2. Schematic of what is seen inside of an oil pipeline. Along with the crude oil, there can be gas (methane), water, natural surfactants, and other substances. The surfactants stabilize the droplets of water flowing through the pipeline and because of the presence of methane, hydrates (white) can form at the interface of the droplets. As the hydrates form and begin to agglomerate, they can cause a disturbance in the flow of the pipeline as depicted above. Adapted from Akhfash et al.[19]

Emulsions

The clathrate hydrates in the oil pipeline tend to form at the droplet interface between the oil and water. This is because there are too few water molecules in the oil phase for the cages to form only in the oil.[20] Typically, droplets are stabilized by surfactants, allowing them to retain their shape. Surfactants stabilize droplets in emulsions by adsorbing to the interface of a droplet between two immiscible liquids and reducing the interfacial tension between them. This prevents them from coalescing into two separate liquids. Surfactant molecules are usually amphiphilic, having both a hydrophobic and hydrophilic component. The hydrophobic tail of the surfactant resides in the oil phase and the hydrophilic head resides in the water (figure 3a).[21]

Another way to stabilize two immiscible liquids is by using solid particles, also known as creating Pickering emulsions. Particle stabilizers have received more interest

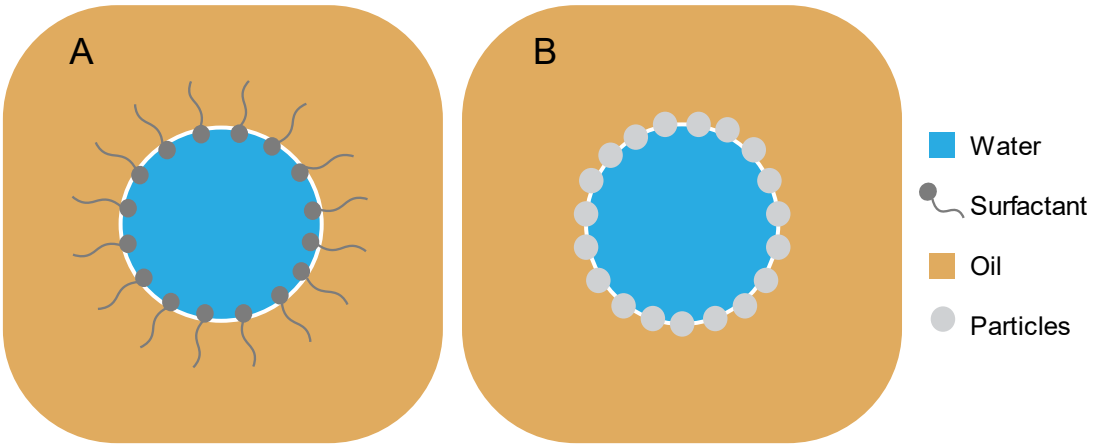

Figure 3. Schematic of A) a surfactant stabilized droplet and B) a particle stabilized emulsion.

in recent years due to their applications in food, cosmetics, oil, and drug delivery.[22] Pickering emulsions stabilize emulsions by creating a steric barrier between the two immiscible liquids, preventing them from coalescing (figure 3b). Particle desorption to a

liquid-liquid interface requires a large amount of energy, meaning it would take a large amount of energy for them to desorb from the interface. This gives particle stabilized emulsions an advantage over ones stabilized using surfactants, which are likely to adsorb and desorb frequently form an interface.[23] The energy required for a spherical particle to desorb form a liquid-liquid interface is shown in Eq. (1):

$$\Delta E = \gamma_{OW}\pi R_{sphere}^2(1 - |\cos\theta|)^2 \quad (1)$$

where γ_{OW} is the interfacial tension, R is the radius of the sphere, and θ is the contact angle of the particle and the interface. In order to find the energy of attachment the sign in the parenthesis would simply be changed to a plus. This equation only holds true for spherical particles, whereas looking at disc or rod-shaped particles would have the energy of desorption calculated using Eq. (2) and Eq. (3) respectively:

$$\Delta E = \gamma_{OW}\pi R_{disc}^2(1 - |\cos\theta|) \quad (2)$$

where R is now the radius of the disc.

$$\Delta E = \gamma_{OW}\pi lq(1 - |\cos\theta|) \quad (3)$$

where l and q are the length and width of the rod respectively. These equations show that the energy required for an aspherical particle to desorb from an interface is much larger, implying aspherical particles could be better for stabilizing emusions.[24]

As seen in Eq. (1-3), the particle wettability plays a major role in the energy of adsorption/desorption of a particle. The particle wettability controls how the particles adsorb to the liquid-liquid interface and what the contact angle, θ, will be. The liquid with less particle wetting ends up being the dispersed phase in the emulsion.[25] When a spherical particle moves from the dispersed liquid to the interface, it will wet to both

liquids. The particles lower the interfacial area by occupying the interface. The energy for the removal of particles from a liquid-liquid interface is higher is typically incredibly high compared to the energy of adsorption, making the particles at the interface incredibly stable.[26] The contact angle is dependent the hydrophobicity or hydrophilicity of the particle. The contact angle helps determine the wettability of the particle.[25] If the particles are too hydrophobic or hydrophilic, they will remain dispersed in only one phase, preventing stabilized emulsions to form. Hydrophobic particles better stabilize water-in-oil (W/O) emulsions while hydrophilic particles better stabilize oil-in-water emulsions (figure 4).[27] The roughness of a particles surface can cause the particle to have an increased natural wettability, meaning a hydrophilic particle would wet more to water than normal and the opposite a hydrophobic particle would wet more to the oil than normal.[26]

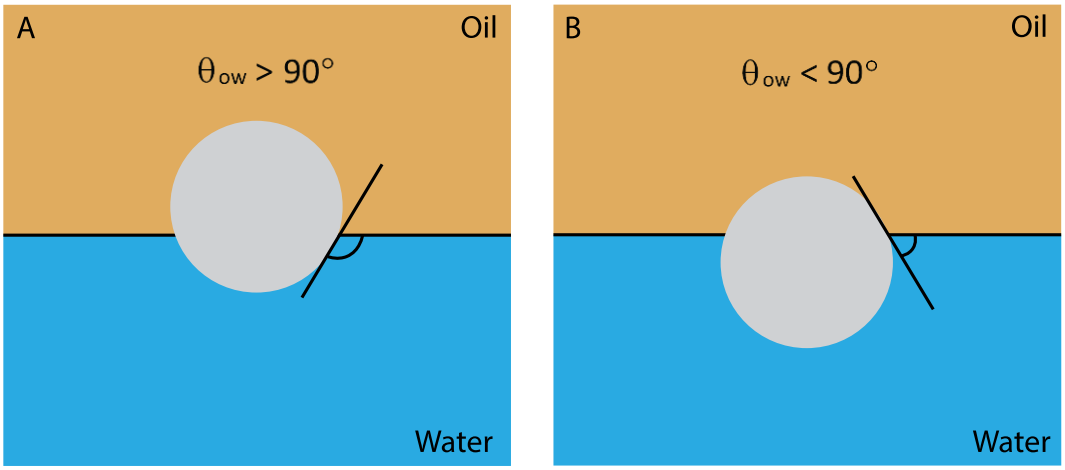

Figure 4. Depiction of the relationship between the contact angle of the particle at the interface and the preferentially stabilized emulsion. A more hydrophobic particle (A) will. The wettability of a particle can be controlled by its hydrophobicity or hydrophilicity. Adapted from Low et al.[24]

The surface and shape of a particle will also have a significant effect on its ability to stabilize an emulsion. The surface of an amorphous silica particle is typically coated

with hydroxyl groups. It can be formed during the particle synthesis as well as from rehydroxylation of the silica.[28] The hydroxyl groups will cause the silica particles to be hydrophilic, causing them to only disperse in the aqueous phase. These particles would need to be functionalized in order to allow for emulsion stabilization. As mentioned before, spherical and aspherical particle adsorption to an interface require a different amount of energy. Spherical particles adsorb to the interface with variance in contact angle, aspherical particles have more variables to look at. In the case of an aspherical particle, the height of the particle becomes important as well as the contact angle. An aspherical particle will lay somewhat parallel to the interface to allow for the maximum interfacial interaction. With a larger interfacial area taken up by these aspherical particles, it makes sense as to why they would be energetically stronger emulsifiers than spherical particles, as shown in Eq. (1-3).

Hydrate Inhibition

A commonly used method of hydrate inhibition in oil pipelines was adding thermodynamic hydrate inhibitors (THIs) into the pipeline.[29] THIs are additives that change the thermodynamics of the hydrate formation, causing them to form at lower temperatures and higher pressures than they would normally. This solution is not an economical solution to the problems plaguing pipelines, as the deeper the pipeline lays underwater, as the cost would increase as more THI is used (figure 5).[30] At least 10 vol % of the THI in water is usually required to effectively combat hydrate formation. Two common THIs are methanol and monoethylene glycol (MEG). These two molecules work

as THIs by competitively binding to the hydrogens in water. The bond between the inhibitors and the water hydrogens is much stronger than the attraction between uncharged molecules, which prevents the bonded water molecules from becoming part of the hydrate structure.[31] Since the methanol and MEG vary in mass, they are each added to the pipeline differently. The methanol is added as a gas to the gas phase in the pipeline, while the MEG is added to the liquid itself to prevent the hydrate formation. Aside from requiring a large amount to be effective, each comes with their own disadvantages. MEG is more widely used as it is less dangerous than methanol. Methanol is also more expensive to recover, further increasing its impracticality. The MEG also faces disadvantages such as a high viscosity with could help reduce flow in the pipeline.[31] Due to the impracticality of using THIs, low dosage hydrate inhibitors (LDHIs) were developed.

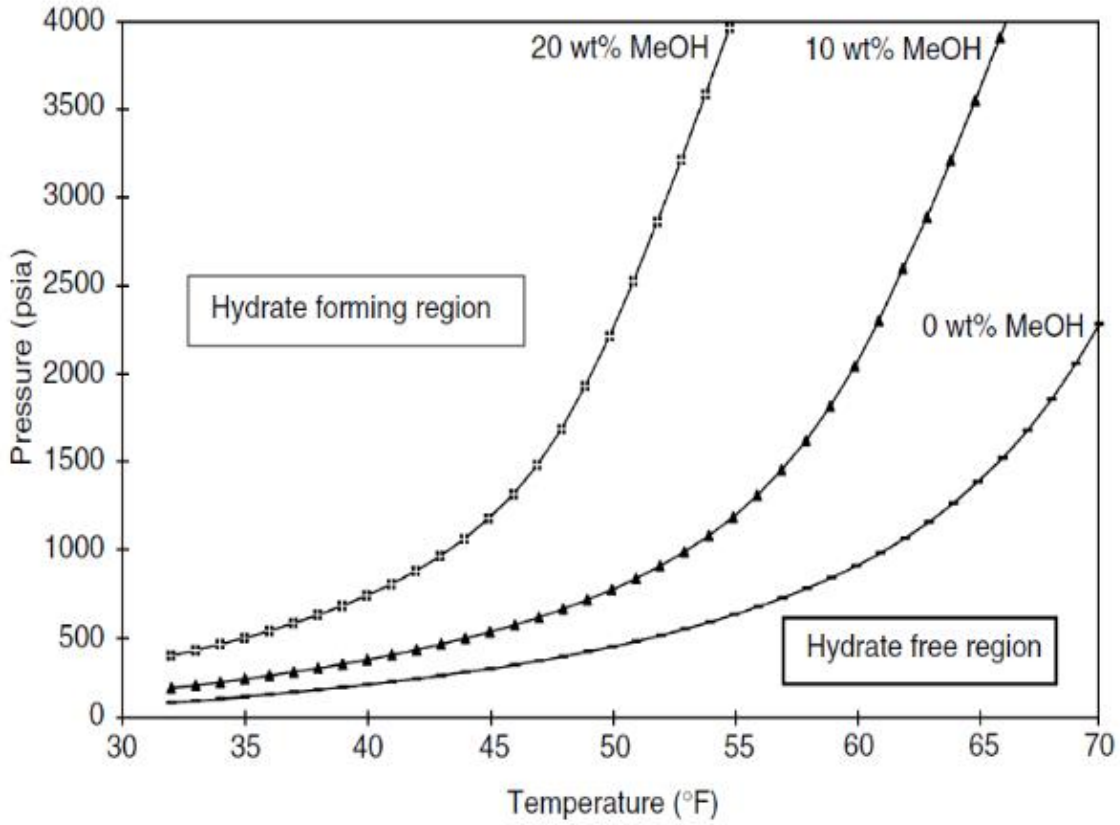

Figure 5. Graph depicting the amount of MeOH needed to prevent hydrate formation at various pressures and temperatures.[32] As the pressure increases and temperature decreases, more inhibitor is required to prevent hydrate formation, making THIs a non-viable solution.

One type of LDHI that has been studied recently are kinetic hydrate inhibitors (KHIs). KHIs work differently in that they work to slow the formation of the hydrates instead of preventing them from forming at all. [33] The goal of slowing the hydrate formation and growth is to allow the oil to pass through the pipeline before the hydrates are developed enough to cause a blockage (figure 7). Since it is an LDHI, much less KHI is required to achieve this goal, making it a more economical solution than using THIs. The downside to this method of inhibition is that it is only temporary, and once enough time passes for the KHIs to be ineffective, there can be a rapid formation of hydrates in the system.[34] While the exact mechanism behind how KHIs slow the hydrate formation is unknown, there are three main theories. One is that they competitively adsorb to the

surface of the crystal, preventing it from continuing to grow. The next is that it binds to the nucleus of the hydrate crystal, thus slowing the growth. The last theory is that they disrupt the water molecules, preventing them from forming into the cage-like structure that makes up the hydrates.[35] Some common KHIs that are studied are polyvinyl pyrrolidone (PVP), polyvinyl caprolactam (PVCap), and polyvinyl pyrrolidone caprolactam (Poly(VP/VC)) (figure 6).

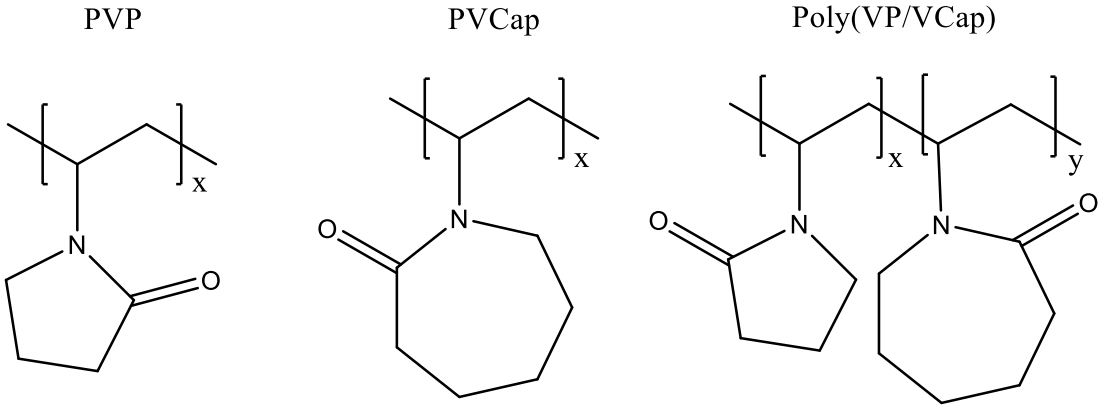

Figure 6. Chemical structures of PVP, PVCap, and Poly(VP/VC). The lactam rings allow binding into incomplete hydrate cages and the hydrocarbon chains help to prevent more cages from forming. Adapted from Palermo et al.[31]

The notable feature shared by all of these polymers is the polyethylene chain with lactam groups coming off the chain. The lactam is important for it is what allows the polymer to attach to the incomplete hydrate cage. The size of the ring determines what structures the polymer can bind to. The attached polymer chains inhibit the growth and formation of the hydrate crystals, reducing the possibility of blockages.[31]

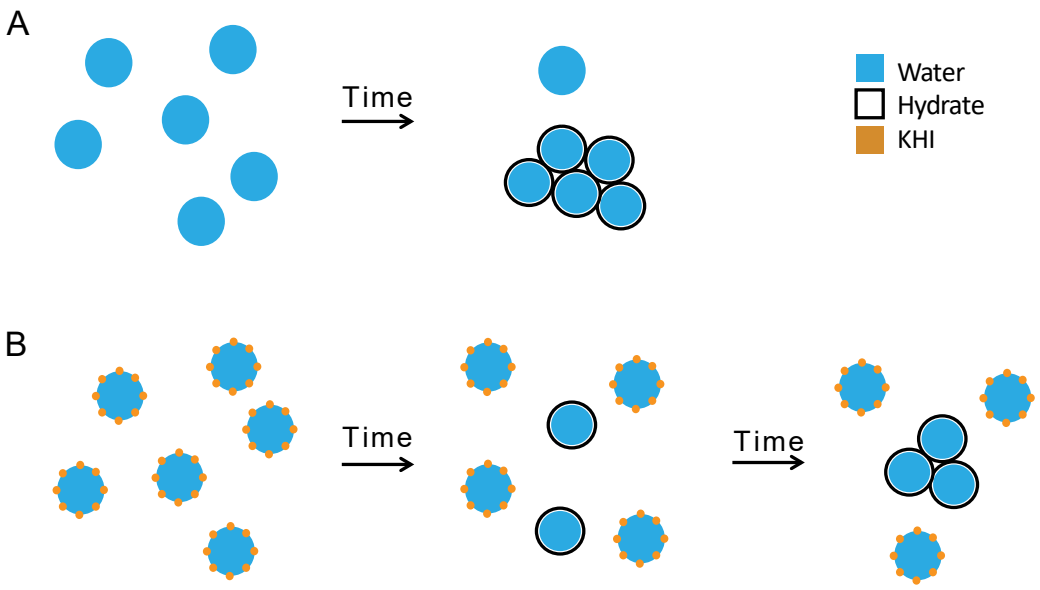

Figure 7. Schematic of the (A) rapid hydrate formation in the absence of any inhibitors and (B) the slower formation of the hydrates over time with the addition of KHI on the particle stabilizers. With a slower hydrate formation, the oil will have more time to move unimpeded through the pipeline.

Anti-agglomeration agents (AAs) work differently than THIs and KHIs in that they work to prevent the agglomeration of the hydrates rather than preventing or slowing the nucleation and growth of the hydrates. AAs interact with the surface of the hydrates that form, allowing for them to act as a steric barrier between the hydrates that form, creating pockets for continuous oil flow.[36] Shell has previously developed AAs that are quaternary salts with two or more n-butyl, b-pentyl, and isopentyl groups. These structures (figure 8) have been found to prevent the growth of hydrates as well as prevent them from coalescing on the wall of the pipeline. The butyl and pentyl groups bind to the holes in the hydrate cage structure, while the tails will prevent continuing hydrate growth. The tails also prevent the hydrates from binding to the walls of the pipeline, and likely serve as a steric barrier between other hydrates that have formed.[33]

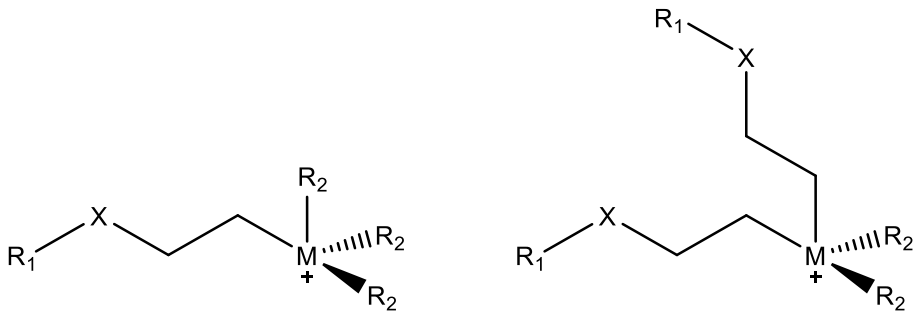

Figure 8. Chemical structures of the quaternary AAs where R_1 is the hydrocarbon tail, R_2 is the butyl or pentyl group, M is N or P, and X is an optional spacer (alkyl chain, nitrogen group, ether group).[33]

Surfactants have been found to act as anti-agglomeration agents[37], but would not be ideal in these clathrate hydrate systems. Surfactants can be toxic and bad for the environment.[38] Since the pipelines being studied are in deep-water locations, it is important to keep environmental impact as low as possible. Another problem with surfactants is that they are incredibly small and they are not permanently adsorbed to the interface. Small AAs will likely not prevent the agglomeration of the hydrates to an effective capacity, still allowing for impedance of flow inside the pipelines. Their desorption could also cause issues as the AA effect would not be stable and, upon the surfactant leaving the interface, gaps formed between the hydrates could be allowed to fill.

A substitute for the use of surfactant as AAs is to use particles that are able to adsorb to the o/w interface and stabilize the emulsions (figure 9b). As mentioned previously, particles are advantageous over surfactants as they are larger and much less likely to desorb from the interface. The larger size offers a much greater barrier between other particle stabilized clathrate hydrates and would allow for more flow through the gaps created. The lack of desorption of the particles from the interface will also cause the

gaps between the hydrates to be stable.

Using Pickering emulsions as a means for preventing hydrate blockages is something that researchers have been increasingly interested in. One study tested the effectiveness of using Aerosil R812 particles, which are hydrophobic fumed silica particles. The results showed that in emulsions consisting of about 10-25% water, a concentration of 0.05-0.5% of particles reduced hydrate formation significantly. At lower concentrations, there were not enough particles to cover the oil-water (o/w) interface, which did not slow hydrate formation. At higher concentrations of particles, the surfactant favored moving to the particles, causing the emulsions to become destabilized.[6] Another study tested the use of Aerosil R974, another type of hydrophobic fumed silica. In this study they looked at the effect of surfactant vs particle stabilization on the droplets for hydrate formation at different water cuts, which denotes the volume of water to the oil. It was found that at smaller sized droplets, the repulsion of the surfactant was stronger than the attraction between the hydrate molecules, causing less of a blockage from forming. The opposite occurred for large water droplets stabilized by surfactant. When testing the solid particle stabilized droplets, there was no decrease in the plugging, due to the strong attractive forces of the hydrates.[39] As shown by these results, using particles as a preventative measure for preventing hydrate buildup can yield both positive and negative results. This is the result of the particles themselves acting as a nucleation site for the formation of clathrate hydrates.[40] In order to use solid particles as a method of hydrate inhibition, it is important to find a way to negate

nucleation at the particle surface from happening.

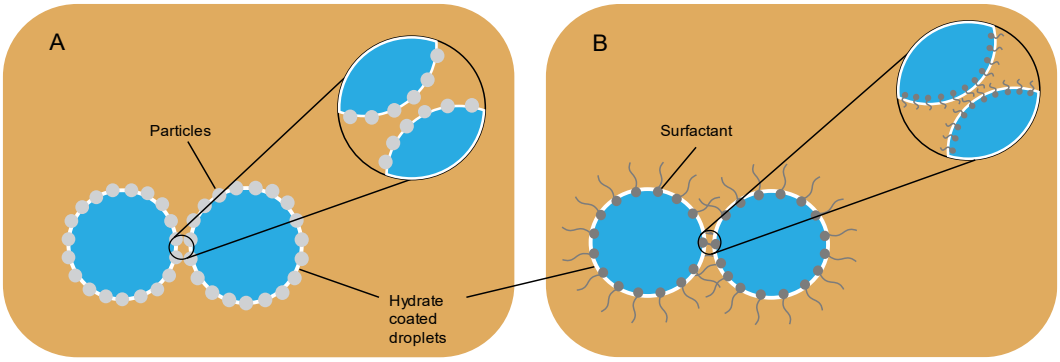

Figure 9: Schematic of (A) particles acting as a steric barrier between hydrates that form at the interface and B) a schematic of the surfactant stabilized anti-agglomeration effect. As the Hydrates form, the gaps left by the AAs allow for oil to continue flowing through with less impedance.

Project Goal

In this thesis we take a new approach to using solid particles as a means to prevent hydrate agglomeration. Established methods in literature have shown that particles can be beneficial as AAs, but can cause hydrate nucleation to occur at a faster rate than normal. By functionalizing our solid particles with kinetic inhibitors, such as PVP, we hope that we can eliminate the weaknesses of each individual method. The PVP will act as a hydrate formation inhibitor that will prevent nucleation at the particle interface, while solid particles act as the AA due to their steric bulk. The PVP will not be able to prevent hydrate formation for an extended period, but if it can slow the hydrate formation enough that the oil can pass through the pipeline before there is a significant blockage. The goal of these experiments will be to test the efficacy of using solid particles functionalized with kinetic hydrate inhibitors to account for the weaknesses each method has individually.

Chapter 2: Experimental Methods

Experimental Techniques

This chapter will discuss the techniques used to functionalize hydrophobic silica particles with the ability to inhibit hydrate blockages as well as the methods used to create our emulsion systems. Information on the materials and equipment will be communicated as well in the following sections.

Chemicals Used

Cyclopentane (Beantown Chemicals, 99%), hexane (MP, 99.9%), acetone (Fisher Chemical, 99.5%), HDK S13 fumed silica (Wacker Chemie, 99.8%), trimethoxyhexadecyl silane (85%), n-octyltriethoxysilane (across organics, 97%), Span 65 (Merck), Span 80 (TCI, 99%), n-vinyl-pyrrolidone (Chem-Impex, 99.5%), ammonium hydroxide (GR ACS, 28-30%), sulfuric acid (Millipore Sigma, 95-98%), hydrogen peroxide (ACS, 30%)

Particle Functionalization

Vinyl Silane Functionalization. All particle functionalization started using HDK S13 fumed silica particles. The particles are amorphous and have a BET-surface area of 110-140 m^2/g. In a 25mL round bottom flask, 250 mg of the S13 particles were dispersed in 10 mL of acetone in a bath sonicator. 30 wt% ammonium hydroxide in water, 100 µL, was added to the reaction flask along with varying amounts of vinyltriethoxy silane (100-1mL) to vary the degree of functionalization. The flask was sealed with a rubber septum and left to sonicate for 1-24 hours depending on the experiment. The solution was diluted with acetone to the 40 mL mark, and centrifuged at 7,100 RCF for 10 minutes, after which

the supernatant was discarded. The pelleted particles were then redispersed in acetone using probe sonication. The acetone rinse and centrifugation were repeated twice more. The resulting particles were left to dry for at least 4 hours at room temperature to yield the vinyl-functionalized particles (Figure 10A)(Appendix, Table 1).

PVP Functionalization. The vinyl-functionalized particles were dispersed in 2 mL of *N*-vinyl-2-pyrrolidone using gentle probe sonication, followed by the addition of benzoyl peroxide, 20 mg. The vial was purged with nitrogen, capped, and heated while stirring in an oil bath at 90°C for 24 hours. The solution was diluted with acetone and centrifuged with 2 repetitions, the same as the vinyl-functionalized particles (Figure 10A)(Appendix, Table 1). The functionalization being used was derived from literature.[41]

Hydrophobic Functionalization. Hydrophobic particle functionalization was achieved by adding a trimethoxyhexadecyl (hexadecyl) or octyltriethoxy (octyl) silane to the particle (Figure 10 B,C). In a 25mL round bottom flask, 250 mg of HDK S13 particles were dispersed in 10 mL of either acetone or hexanes, depending on the degree of functionalization, using a bath sonicator. 30 wt% ammonium hydroxide in water, 100 µL, was added to the reaction flask along with varying amounts of hexadecyl silane (100-1000 µL) to control the hydrophobicity. The flask was sealed with a rubber septum and left to sonicate for 1-24 hours depending on the experiment. The solution was diluted with acetone to the 40 mL mark, and centrifuged at 7,100 RCF for 10 minutes, after which the supernatant was discarded. The pelleted particles were then redispersed in acetone using probe sonication. The acetone rinse and centrifugation were repeated twice more. The resulting particles were left to dry for at least 4 hours at room temperature to yield the

hydrophobic functionalized particles (Appendix, Table 1). These particles could then be functionalized with PVP as well using the vinyl silane and PVP functionalizations discussed above. 300 µL of the vinyltriethoxy silane and 2 mL of the PVP were used to functionalize these particles.

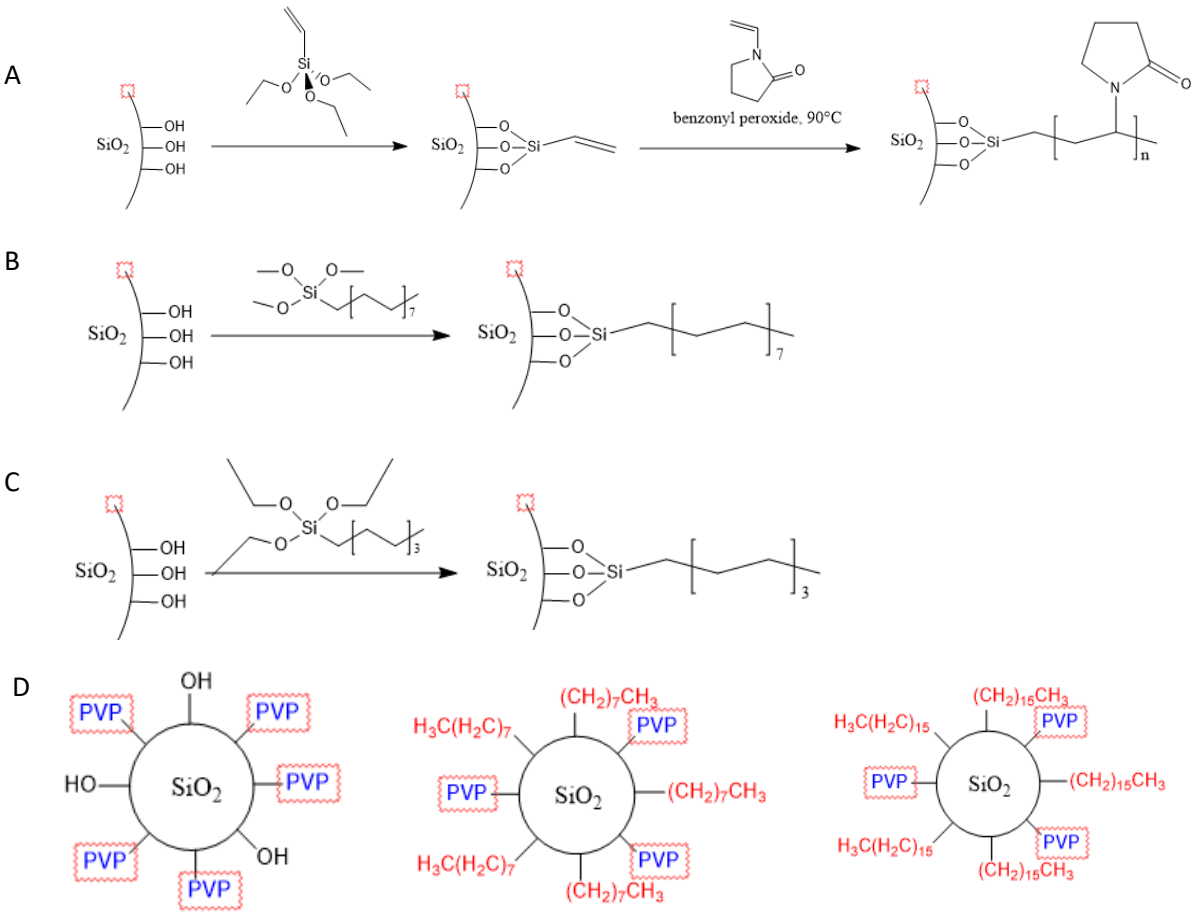

Figure 10. Reaction scheme of the A) particle functionalization with pvp only, B) the particle functionalization with a hydrophobic silane group (trimethoxyhexadecyl silane), and C) the particle functionalization using a hydrophobic silane (octyltriethoxy silane). D) Particle surface fuctionalized with only pvp (left), with both pvp and trimethoxyhexadecyl silane (middle), and with both pvp and octyltriethoxy silane (right).

Emulsion Formation

Surfactant Stabilized Droplets. Span 65, 0.1 g, was dissolved in cyclopentane, 9.9 g, to make a 1 wt% surfactant solution. 100 µL of DI water was added to 1 mL of the cyclopentane surfactant solution and then vortexed at the highest setting to create the desired droplets.

Surfactant and Particle Stabilized Droplets. For these droplets, various types of particles (table 1) were dispersed in water or cyclopentane using probe sonication with varying concentrations (0.1-10 wt%). The same 10:1 ratio of cyclopentane to water mixture was made and vortexed to achieve the desired droplets.

Particle Stabilized Droplets. Hydrophobic particles functionalized using the hexadecyl and octyl silanes were dispersed in either cyclopentane or water with varying concentrations (0.1-2 wt%) using probe sonication. Mixtures of both cyclopentane in water and water in cyclopentane were made in 10:1 ratios as done previously and were vortexed to achieve the emulsification.

Treating Glass Slides

The glass slides typically used in the metal dishes caused droplet pinning to occur on the glass. This is detrimental in the analysis as there is a good chance for the glass to affect the rate of the hydrate growth and nucleation. In order to prevent the pinning, the glass was cleaned to ensure they were completely clean beforehand. The glass slides were each pre-rinsed with water and acetone before being placed in piranha solution to ensure everything on the surface of the glass was removed. The piranha solution was made with

a 3:1 volume mixture of sulfuric acid and 30 % hydrogen peroxide. The glass slides were left in the solution for no longer than 1 hour before being removed and rinsed one final time to remove the residual piranha. The piranha cleaned slides were only used one time each to prevent contamination between trials.

Experimental Apparatus

Optical Microscope. Optical microscopy was the main method of visualization of the hydrate formation at the droplet interface. Two microscopes were used for this analysis, one being a Nikon Eclipse Ts2 and the other a Nikon Eclipse Ti. The Nikon Eclipse Ts2 was the main one used and allowed for magnification between 4-20x. A camera attachment (Imagesource) fed the images from the microscope to a computer using bright field microscopy. This is a simple form of microscopy where a white light shines on the object and the camera records the contrast of the light on the sample. This microscope recorded videos in black and white. The Nikon Eclipse Ti used a zyla camera attachment and allowed for some clearer videos, more modification of the recording, and a magnification up to 40x, but was not necessary for a majority of the videos taken. The microscopes were used to observe the dishes containing the hydrate solution and recorded the hydrate formation process. The videos recorded lasted anywhere between 10 minutes to 5 hours depending on the method of inhibition being tested.

Temperature Stage. Since the hydrate formation occurs at lower than room temperature, the dish was placed in a temperature stage. The temperature stage used was an Instec TSA12Gi stage. It allowed for a temperature control range of -25 to 90°C,

which was important for maintaing a constant temperature for the duration of the hydrate formation. The temperature was kept constant, kept from overheating by the connected water cooler (brand) which pumped room temperature water through the stage. The dish was placed inside the chamber which was sealed to prevent fluctuations in temperature from the surrounding environment. The temperature stage was kept at 2°C to ensure only hydrates formed and not simply ice. There were some periods of times when there was noticeable condensation on the glass windows, which was solved by purging the chamber with nitrogen or compressed air.

Characterization

Thermogravimetric Analysis. Thermogravimetric analysis (TGA) is a technique used to measure the components and thermal stability of a material. TGA plots the weight % of a substance over a temperature range. In TGA analysis, a material is heated up and the loss of mass is recorded as the temperature increases. By analyzing the weight loss through decomposition, we could determine if the desired components were in the material. This will be useful when analyzing the amount of PVP on the surface of the particles after the functionalization, however the amount of each silane will not be easy to determine using this method as they would decompose at similar temperatures. The TGA used to analyze the hydrates was the Discovery Series TGA Q5500 from TA instruments. Platinum high temperature pans were used to assess the mass loss of the functionalized silica. The parameters set for the analysis was a 10°C/min ramp from 25-120°C and held in an isotherm for 10 minutes to make sure all solvent was evaporated.

The ramp rate was raised to 20°C/min from 120-800°C for decomposition of the surface organic groups. The analysis was done under air, so it was not a "controlled" decomposition as it didn't matter the order in which the functional groups were burned off.

Rheometer. Rheological analysis will be the most important method of analyzing the agglomeration of the hydrates. As the hydrates form and cluster together, it is important to know the rate at which the agglomeration is causing a slowing or stoppage of movement in a given system, and the rheological analysis of the system will be integral for this. The rheometer used in our testing was a Discover HR-3. The device uses various shaped rotors to apply a shear stress to a system, giving an analysis on the viscoelastic change over time for a given system. There is a cup in which a liquid solution can be placed, and the shearer is lowered inside. Two geometries were tested in our experiments; a concentric cylinder and a vane geometry (figure 11). The rheometer was run with a shear rate of 10 s^{-1} for all of the samples and they were tested with water cuts between 10-40 vol %. The result of the rheological analysis is a plot of the viscoelastic change over time. An increase in viscosity over time or a sudden stoppage of the curve would likely indicate hydrate formation in the system.

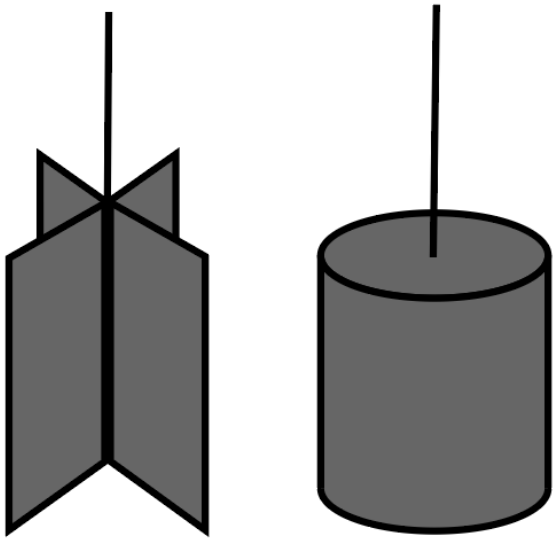

Figure 11. Schematics of the vane (left) and concentric cylinder (right) geometries tested in the rheological analysis.

Chapter 3: Results and Discussion

Choosing a Surfactant

Hydrates form at the o/w interface which are abundant in droplet systems. Water-in-oil droplets are stabilized in oil pipelines, stabilized by natural surfactants and particulates. In order to analyze this hydrate formation, it was important to first find a suitable stabilizer. Span 80 (0.1-1 wt % in CP) was the surfactant that was typically used when analyzing water-in-cyclopentane hydrate systems and was the first surfactant we tested. Span 80 stabilized droplets were unstable and rapidly coalesced rapidly. This may be due to our continuous phase being only cyclopentane, rather than a mixture of oils. Span 65 (0.1-1 wt % in CP) was able to stabilize the water-in-cyclopentane droplets well, and thus the surfactant used to stabilize the emulsions in future trials. The concentration of surfactant was seen to have a negligible effect on the hydrate time of formation, and thus Span 65 was chosen as the droplet stabilizer for our system.

Observing Hydrate Formation

In order to collect data on the clathrate hydrate formation in our system, it was important to first define the onset time of formation and the end of the hydrate formation/growth. In our analysis of the hydrate formation, we used optical microscopy to visualize the hydrate formation. Since the system lies undisturbed on the microscope, the droplets lie still and do not agglomerate as they may in a moving system. The initial onset of formation was recorded at the point when there was a noticeable crusting on the surface of the droplet. Over time the crusting was observed to intensify and grow. As

the hydrates formed and began to grow, the droplets began to be deformed from their spherical shape. The end time of the hydrate formation/growth was noted at the point in which no change was seen in the hydrates that formed. The initial time of formation was usually between 5-15 minutes for most trials and was sometimes difficult to accurately determine due to small changes on the droplets that could have mimicked hydrate formation. End time of formation was a better metric of hydrate formation in the system as there was a greater variance in time. This allowed us to determine which systems had better or worse inhibition.

The initial visualization of the hydrate formation times was done using only a water-in-cyclopentane emulsion stabilized by Span 65. As seen in figure 12, the droplets at time t=0 are spherical and contain smooth surfaces. At time t=1200 s, the droplets begin to show crusting at the interface, signifying the formation of hydrates in the system. At this point in time, the hydrate formation is only beginning and the crusting seen on the droplets is light. At time t=3600 s, there is a noticeable hydrate formation in the droplet system. Each droplet has significant hydrate coverage which can be seen by the strong deformation as the droplet interface.

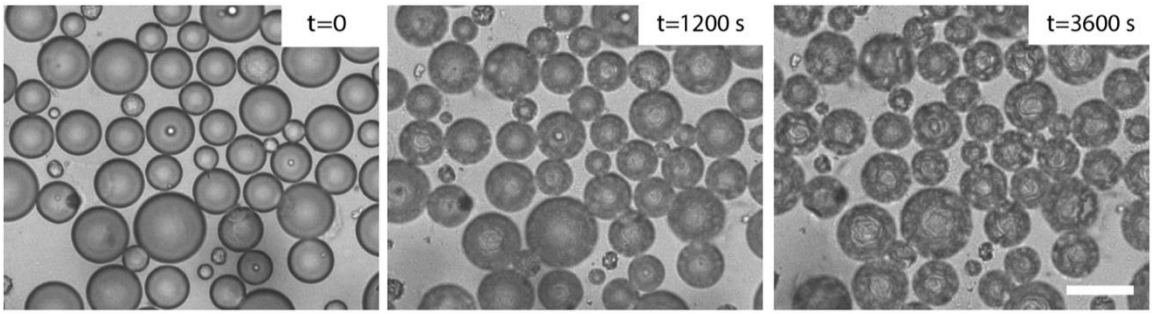

Figure 12. Series of photos taken of the water-in-cyclopentane, scale 100 µm. The droplets start out as smooth spheres, and over time a crusting can be seen at the surface indicative of hydrate formation. The hydrate induction time was noted when hydrate crusting is first seen and the end time of formation was when there was no more noticeable change in the system.

Observing Hydrate Formation in Surfactant Stabilized Solutions

In order to set a standard for hydrate formation times, the first set of trials looked at hydrate formation times in a surfactant only stabilized system. Shown in figure 13 are the induction and end time of the formation of hydrates in both a 0.25 and 1 wt % surfactant solution. The data (Appendix, Table 2) shows that the lower concentration of surfactant led to a more diverse end time of formation for the hydrates, ranging from anywhere between 60 -120 minutes. It is likely that the end time of formation for trial 2 is simply an outlier due to the volatility of the hydrate system. The majority of the trials lead to an end time of formation around the 60-minute mark, which likely shows a more accurate representation on the effect of the hydrate formation with only surfactant molecules present in the system. The end time of formation for the 1 wt % Span 65 solution was found to be consistent across the trials conducted, and therefore became the basis for comparison to the particle systems tested.

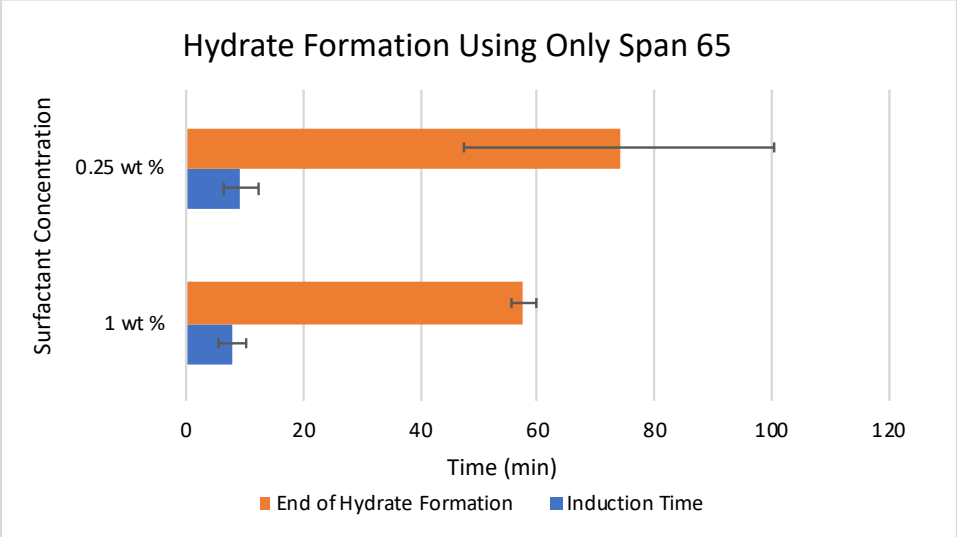

Figure 13. Induction and end time of hydrate formation for a surfactant only system. 1 wt % Span 65 in CP was used as the surfactant stabilizer in this system. The surfactant was dispersed in the CP and the dispersed phase was DI water. The end time of formation using 0.25 wt% Span 65 was much more sporadic compared to the 1 wt %, and thus the 1 wt % solution became the standard used for future experiments.

Adding Particles to the System

In order to test the effect of hydrate formation in the presence of particles, S13 fumed silica was added to the system in addition to the surfactant. Due to the hydrophilicity of the particles, the droplets could not be stabilized without the surfactant in the solution. The particles were dispersed in the water phase at various concentrations to see their effectiveness as hydrate inhibitors. The droplet solutions made were a 10:1 vol ratio of cyclopentane to water. The particle concentrations were varied between 0.1 – 10 wt % of S13 particles dispersed in the water phase. As shown in figure 14 and table 2, the particle concentration seems to have negligible effects on the hydrate formation. The hydrate induction time for the particle systems lies around the 4–6-minute mark of the recordings, which seems to be slightly lower than the times seen without any particles. The end time of formation on average lies between the 50–60 minute mark for the majority of the trials. Some of the runs showed that the hydrate formation took longer than the length of the recording (60 minutes), but had incredibly small changes signifying the hydrate formation was close to completion. The 0.1 wt % particle solution appeared to have a large standard deviation, which could be caused by the small number of particles in the system. There are too few particles for a significant hydrate inhibition but, depending on the dispersion in each individual trial, there could have been slight differences in the outcome of the hydrate formation times. It is also possible that the hydrate formation times could have been different simply due to the volatility of the hydrate systems. The 4 wt % and 10 wt % systems stood out and showed a significant inhibition in the hydrate systems. As a hydrophilic particle, it makes sense that higher

concentrations had a stronger effect on the hydrate inhibition. The 6 wt % system stands out as an outlier to this expectation and rules out this trend. The S13 particles appeared to only be effective inhibitors for the 4 wt % and 10 wt % systems, potentially due to to little particles in the lower concentration systems. It is possible the 6 wt % system exists as an outlier.

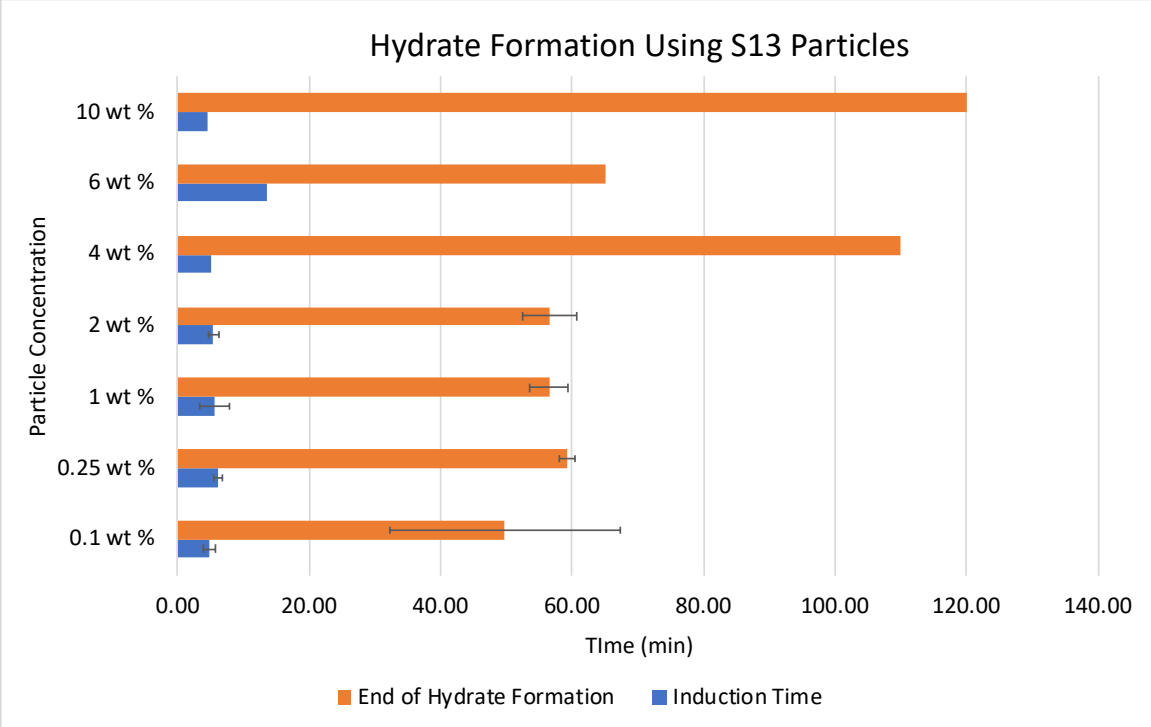

Figure 14. Average induction and end time of formation for hydrate systems with both S13 fumed silica particles and surfactant. The systems tested used 1 wt % Span 65 in CP as a stabilizer and the S13 particles were dispersed in DI water which was the dispersed phase. The most effective inhibition is seen around the 4 and 10 particle wt % solutions, with the 6 wt % seemingly an outlier to the trend.

Increasing Particle Hydrophobicity

In order to get the S13 particles to adsorb to the o/w interface, it was necessary to increase the hydrophobicity of the particles. The S13 particles were functionalized using hydrophobic silanes at various concentrations in order to achieve this. The silanes

used were hexadecyl silane and octyl silane. The particle wettability changed depending on the functionalization solvent and concentration of silane used. Hexanes and acetone were used as the functionalization solvents, but acetone became the standard for functionalizing the particles as it decreased the degree of functionalization compared to the hexanes. The particles functionalized using the hexanes ended up being too hydrophobic, and the silane concentration could not reliably be reduced further. Using acetone caused there to be a lower increase in the hydrophobicity, and led to particles that were better able to adsorb to the o/w interface.

The fist silane tested was the hexadecyl silane. At higher amounts of hexadecyl silane used in the hexane functionalization, 250 µL – 1 mL of the silane, the particles were too hydrophobic, becoming completely indispersible in the water phase. The particles were dispersible in the cyclopentane but failed to stabilize any droplets without surfactant present. The particle hydrophobicity needed to be reduced as they were likely trapped in the oil phase, facing the same problems faced with the S13 particles being stuck in the water. When the solvent was changed from hexanes to acetone, the 250 µL hexadecyl silane functionalized particles were closer to the desired wettability as the particles sunk in the water but could not be dispersed well in either phase. The particles functionalized with 50 and 100 µL hexadecyl of the silane showed some promise in stabilizing the water-in-cyclopentane emulsions without the need for surfactant. The 50 µL hexadecyl silane functionalized particles showed some droplet stabilization, but a lot of gelation in the dish (figure 15). There were some stable droplets, although they were not spherical in shape like what was seen with the surfactant stabilized systems. The 100

µL hexadecyl silane functionalized particles showed some stabilization, but had less stability than the lower functionalization and still showed the gelation in the system (figure 16). None of the hexadecyl silane functionalized particles were found to be effective particle stabilizers due the inconsistent ability to stabilize droplets in the hydrate system, if at all, and since they caused gelation which impeded the ability to visualize hydrate formation.

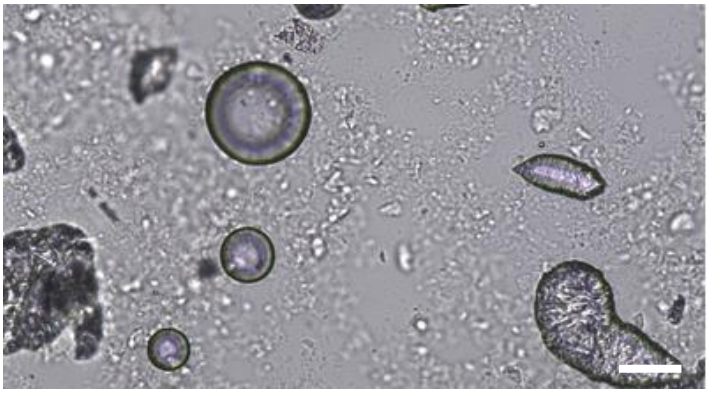

Figure 15. Droplet system using 1 wt % particle 1 (Appendix, table 1) in CP as the droplet stabilizer. Some amorphous droplets are present in the solution, but they are unstable and surrounded by gelation which inhibits visualization of the system, scale 100 µm.

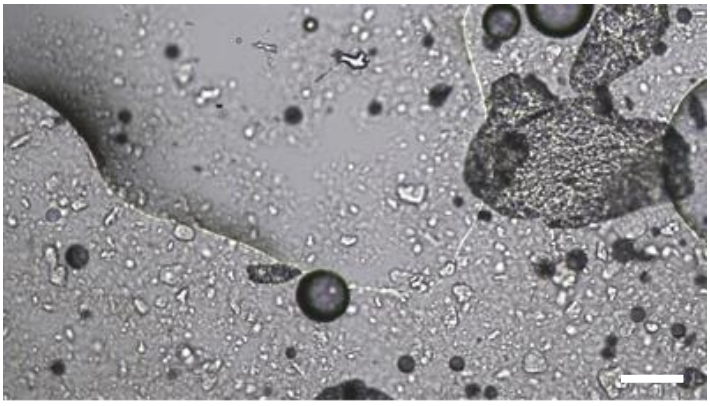

Figure 16. Droplet system using 1 wt % particle 4 (Appendix, table 1) in CP silane as the stabilizer. The droplets were unstable and coalesced rapidly and had the same gelation as the sample seen in figure 15 above, scale 100 µm.

The other silane we tested was the octyl silane. All of the functionalized particles for this were made using acetone as the solvent. The higher concentrations of octyl silane

tested, 500 µL – 1.25 mL, made the particles too hydrophobic and caused the particles to stay in the oil phase. At the low end of the octyl silane concentrations, 50 - 150 µL, the particles were slightly dispersible in the water phase, but still could not stabilize the emulsion. They were still too hydrophilic, unable to be dispersed in oil. These particles were unable to stabilize the droplets in the system, likely because the particles were stuck in the water. At 200 and 400 µL of octyl silane functionalization, the particles were somewhat able to stabilize the droplets (figure 17), although the droplets agglomerated. The problem with the 200 and 400 µL of octyl silane functionalized particles was the particle dispersion only worked a fraction of the time in either system, and even then, the droplet stabilization was not guaranteed. Due to the inconsistencies of this system and time constraints, a useful particle functionalization was not found and more testing will need to be done to get the particles to a state of consistent emulsion stabilization.

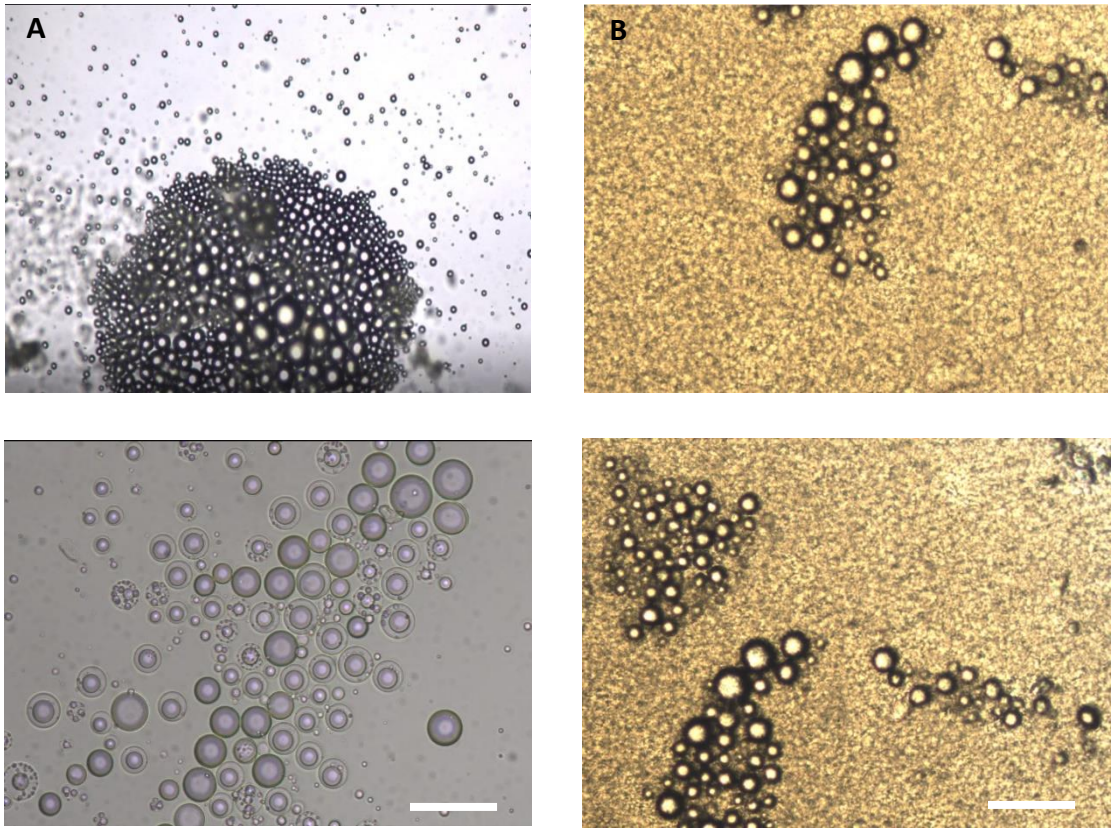

Figure 17. Droplets stabilized using A) 0.05 wt % particle 24 (Appendix, table 1) in cp and B) 1 wt % particle 27 (Appendix, table 1) in cp. Both systems showed stabilized droplets, but were inconsistent in the formation. The difference in color stems from one being an oil-in-water emulsion and the other a water-in-oil emulsion, scale 500 µm.

In order to analyze the effect of the silane particle functionalization on the hydrate formation, it was necessary to have surfactant present in the system to stabilize the droplets. The results of this system were compared to the S13 particle system and the Span 65 system to visualize the effect of the added silane. The particles tested were only those functionalized with the vinyltriethoxy silane, using 100 µL, 500 µL, and 1 mL for the functionalization as the controls. Each degree of functionalization was tested at multiple particle concentrations ranging between 0.1 -10 wt % (figure 18), the data for which can be found in Table 4 of the appendix.

The effectiveness of the particles changed slightly dependent on the amount of

vinyl silane used for the functionalization and the concentration of particles used. The 100 µL vinyl functionalized particles were slightly more effective than the basic particles were at 0.1 wt % and above 4 wt %., with a maximum end time of formation around 80 minutes. The particles with only 100 µL vinyl functionalization were hydrophilic and dispersed easily into the water. The 0.1 wt % concentration appeared as an outlier for this degree of functionalization as it would be expected that too little particles were in the system to be effective. The uneven dispersion of particles and the volatility of the system could be causing the irregularity in effectiveness if there aren't enough particles at or near the interface to inhibit the hydrates properly.

The 500 µL vinyl silane functionalized particles showed some improvement over unfunctionalized particles as well, but by no large amount. The trend for this degree of functionalization followed similarly to what was seen with the 100 µL vinyl functionalized particles, but the end time of hydrate formation for this system was a bit higher. The wettability of the particles could have changed slightly, causing the 500 µL vinyl silane functionalized particles to be slightly more effective. Both systems see only a slight hydrate inhibition effect from the particles mainly appear to be most affected by the Span 65 surfactant molecules. The trends seen could end up simply being coincidental and not indicative of an actual trend in the inhibition.

The 1 mL vinyl silane functionalized particles showed some improvement in the hydrate inhibition, but only for the lower concentrations. At concentrations above 1 wt %, the end time of hydrate formation was around 70-75 minutes, which only showed a slight improvement over the surfactant only system. The best inhibition was at 1 wt % of

the hexadecyl silane functionalized particles. The particles were likely able to adsorb in some capacity to the o/w interface, blocking the nucleation sites of the hydrates, while not having enough particles in the system acting as nucleation sites to increase hydrate formation times.

The results for the vinyl salinized particles show hydrate formation times scattered. Upon testing some of the concentrations a multitude of times, it can be seen the formation times can have high standard deviations, likely due to the volatility of the system. The discrepancy in the data could also be caused by the use of the optical microscope and only having visualization of hydrate formation. By using DSC or rheological analysis, more accurate measurements could be made to give a clearer trend for the hydrate formation.

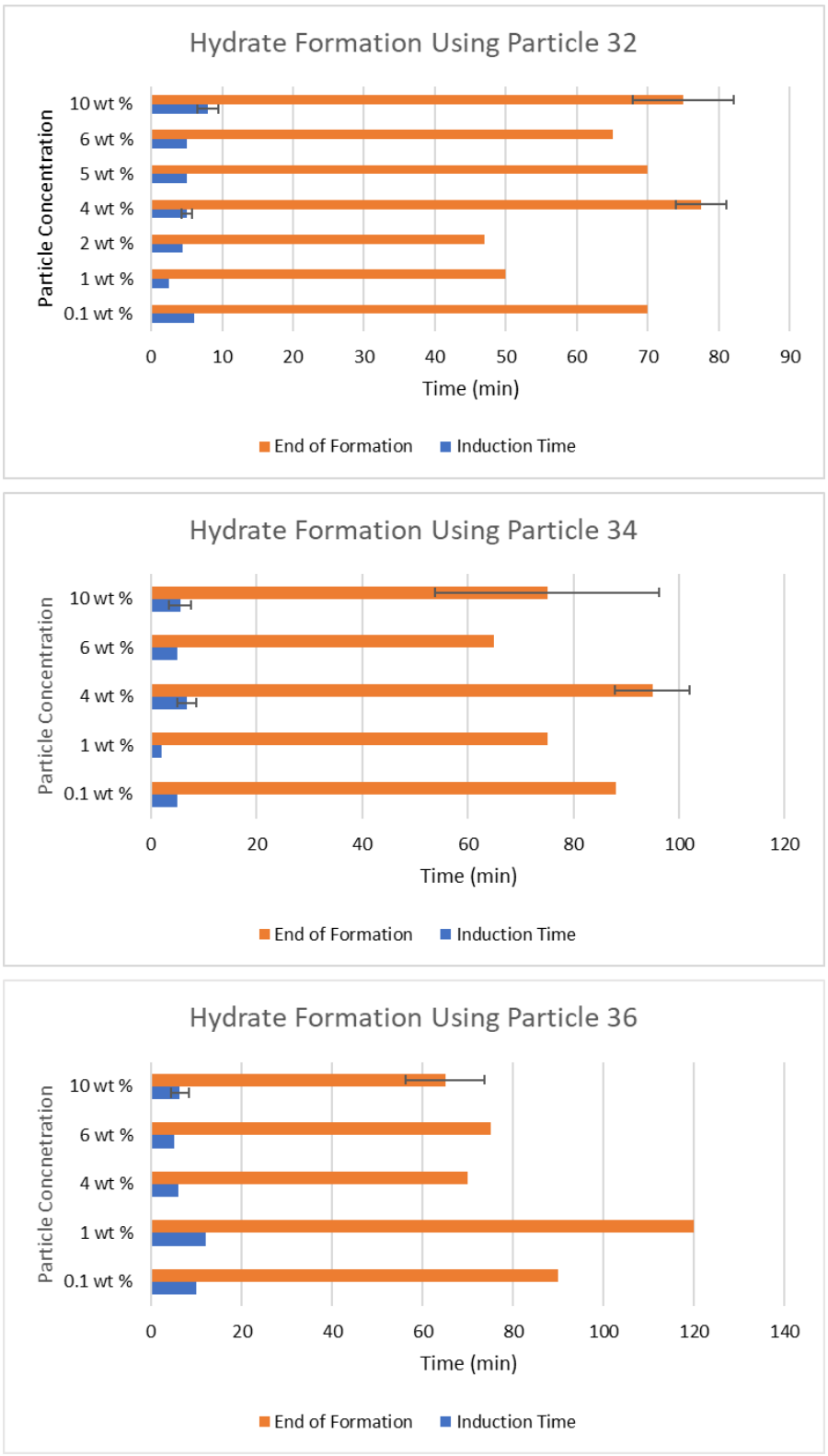

Figure 18. Hydrate induction and end time of formation at varying vinyl silane functionalizations and particle concentrations (Appendix, Table 1). The particles are dispersed in the cyclopentane with DI water as the dispersed phase. The droplets were stabilized using 1 wt % Span 65 in CP.

Testing PVP as a Hydrate Inhibitor

Since PVP is a known kinetic hydrate inhibitor, by adding a PVP functionalization to the particles, they would hopefully have an increased hydrate inhibition effect in addition to the anti-agglomeration effect. The S13 fumed silica was functionalized with varying amounts of PVP. Since kinetic inhibitors are low dosage, the goal was to use low concentrations of the PVP to determine if they would be effective as an addition to the particles.

The first thing that was tested were the PVP only controls that had the PVP dispersed in the water and with surfactant to stabilize the droplets. Each concentration was tested a minimum of 3 times for the inhibitive effect and the hydrate formation times were averaged together. The data (Appendix, Table 5) showed that the addition of only PVP in the solution had a minimal effect on delaying the hydrate formation (figure 19). The PVP only seemed to delay the end time of formation by 5-20 minutes for all of the concentrations tested. This is slightly unexpected for the hydrate system but it may also be because this system is different than a methane hydrate system typically seen in pipelines

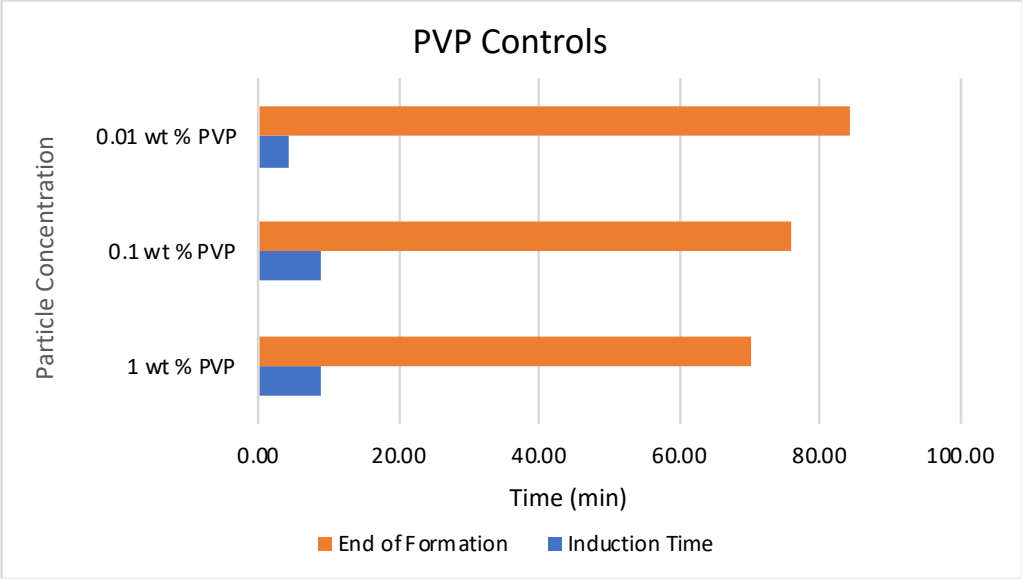

Figure 19. Average induction and end time of formation for hydrate formation in PVP and surfactant solution. The PVP was dispersed in the water, which was the dispersed phase. The droplets were stabilized using 1 wt % Span 65 in CP.

The vinyl silane functionalized particles were next functionalized with PVP to test the effect of both inhibitors in one system. The systems tested had 100 µL, 500 µL, and 1 mL vinyl silane and were each functionalized in 2 mL PVP each. Since the vinyl silane would control the degree of PVP functionalization, it was important to have various silane controls to be able to test multiple amounts of PVP. The particles alone were unable to stabilize the droplets and thus 1 wt % Span 65 in CP was used as the continuous phase. The hydrate induction times for these systems were extremely difficult to discern and thus only then end time of formation is shown (figure 20).

The inhibitive effect of the silane and PVP functionalized particles was significant at some concentrations compared to the unfunctionalized particles. The 100 µL vinyl silane and PVP functionalized particles had a large impact on hydrate formation at 4 and 10 wt % of particles. This system is hydrophilic, so a higher concentration of particles

causing inhibition of hydrates is expected. The 4 wt% particle solution prevented the hydrate formation by about an hour when compared to the 10 wt % system, which inhibited hydrate formation by 40 – 60 minutes compared to the S13 particle system. The 0.1 wt % showed some hydrate inhibition with a 30-minute delay on the end time of formation as well. The 1 wt % system showed a relatively low-end time of formation at 50 minutes.

The 500 µL vinyl silane and PVP functionalized particles also showed their best performance around 4 and 10 wt % with a hydrate end time of formation of 180 and 140 minutes respectively, following the expected trend of a hydrophilic system. It is possible these particles were more hydrophilic than the 500 µL vinyl silane functionalized particles due to the addition of the PVP which likely increased the hydrophilicity of the particle. The 6 wt % was found to be an outlier in the data and goes against what the expected trend would be for the system. The volatility of the hydrate formation could be at play here and since these systems only had one data point, more testing is required to determine the issue.

For the 1 mL vinyl silane and PVP functionalized particles, the most significant inhibition was at 0.1 and 1 wt % with hydrate end times of formation of 135 and 120 minutes respectively. The end time of formation almost doubles compared to only using S13 particles, but is not as effective as the lower vinyl silane functionalized particles. The inhibition at lower particle concentrations follows a similar trend seen with the 1 mL vinyl silanized particles with no PVP. At the higher concentrations there is still some inhibitive effect, but is greatly reduced.

The addition of the PVP to the particles appears to have a positive effect on their inhibitive properties. While the particles and the PVP alone were not as effective as inhibitors, the combination appears to have caused a more significant effect on the system. The particles are hydrophilic and have a competitive absorbance with the water molecules, preventing the cages from forming. The PVP might help the particles bind to hydrates that are mid formation as well and have an extra inhibitive effect from the particle and polymer chain.

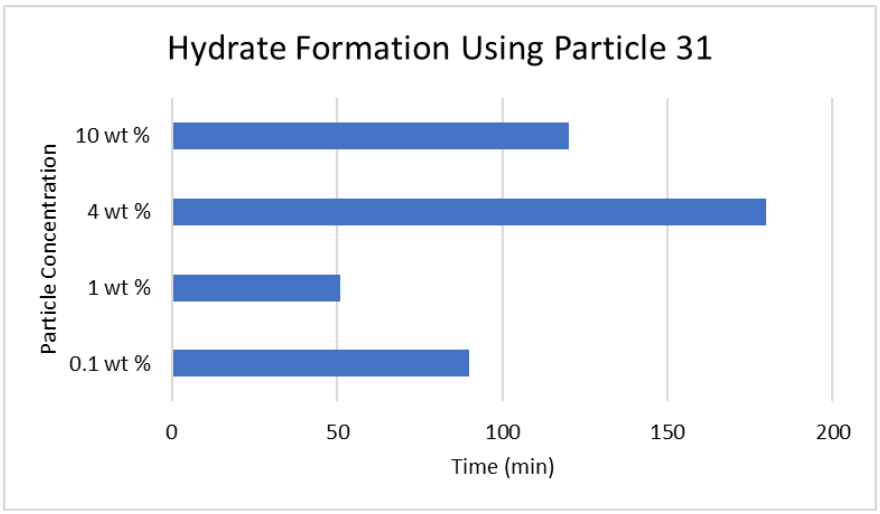

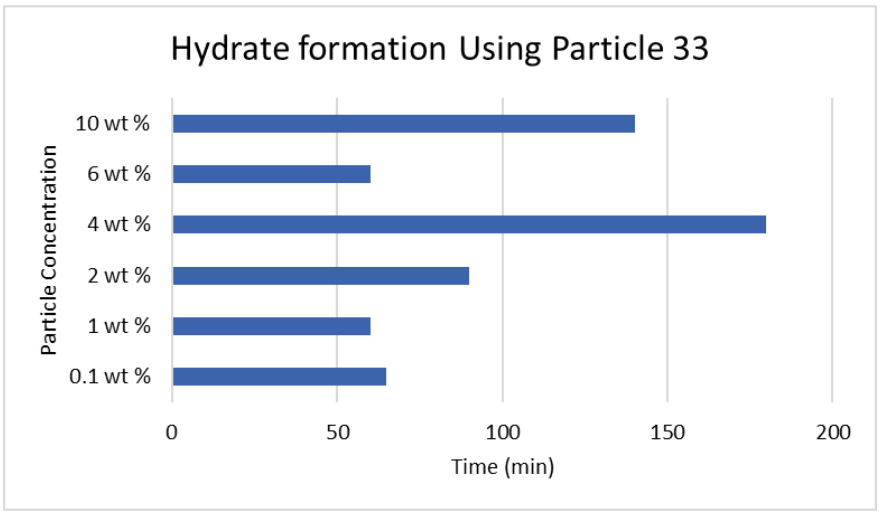

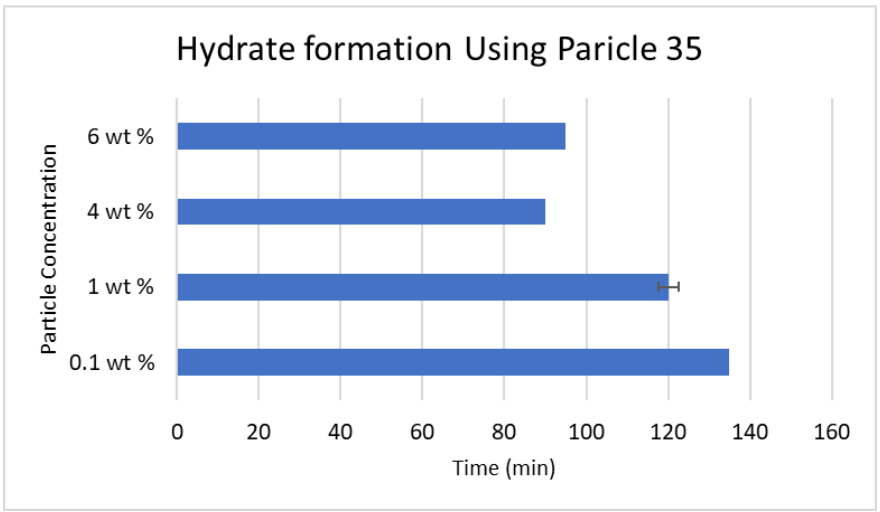

Figure 20. Hydrate induction and end time of formation for particles 31, 33, and 35 (Appendix, Table 1). 1 wt % Span 65 in CP stabilized the emulsion. The PVP functionalized particles were dispersed in the DI water which was the dispersed phase. The effectiveness of the inhibitor appears to be drastically affected by the amount of silane and PVP functionalization as well as particle concentration.

In order to test the effectiveness of the functionalized particles, blind trials were conducted on selected particle concentrations of the 100 µL and 1 mL vinyl silane and PVP functionalized particles that showed extremes in their respective hydrate formation times. The reason for this is that the data could have been skewed due to pre-existing knowledge of the expected trends. Optical visualization of the hydrate formation was difficult, and it was important to mitigate as many factors that could influence the formation times observed. The data from the blind trials showed almost the opposite results as was found in the normal trials (figure 21) (Appendix, Table 7). This likely shows that the systems we tested are somewhat skewed, but are also inconsistent due to the volatility hydrate formation system.

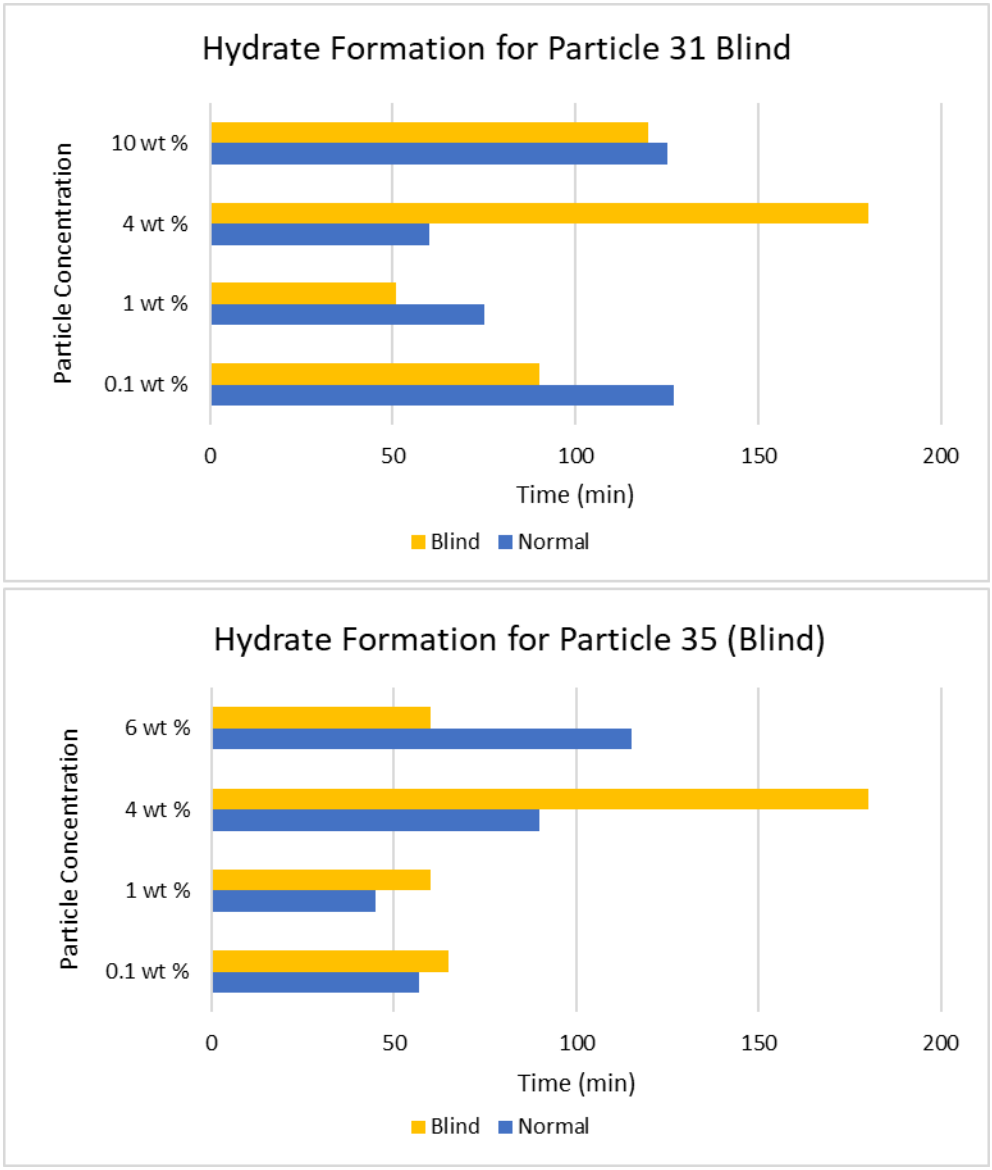

Figure 21. Hydrate end time of formation for the blind trials of particles 31 and 35 (Appendix, Table 1) compared to the results from the normal trial. The emulsion was stabilized using 1 wt % Span 65 in CP and the particles were dispersed in the water. The results of the blind trials show nearly opposite results and trends for the hydrate end times of formation of each set of experiments, despite using the same particles and concentrations.

Confirming the Prescence of PVP on the Particles

In order to confirm that the PVP was present on the functionalized particles, they were analyzed using thermogravimetric analysis. The particles were sampled before and after functionalization to determine the difference in the curves (figure 22). The top graph

shows a slight decline over the temperature increase, signifying there is nothing significant coming off of the particle. The second graph showing the PVP functionalized particles shows a weight loss of around 17 % as the temperature increases. The sharp decline starts around 350°C, which is the expected decomposition temperature for the PVP. Since that was the only change between the runs, it can be assumed that this is the PVP

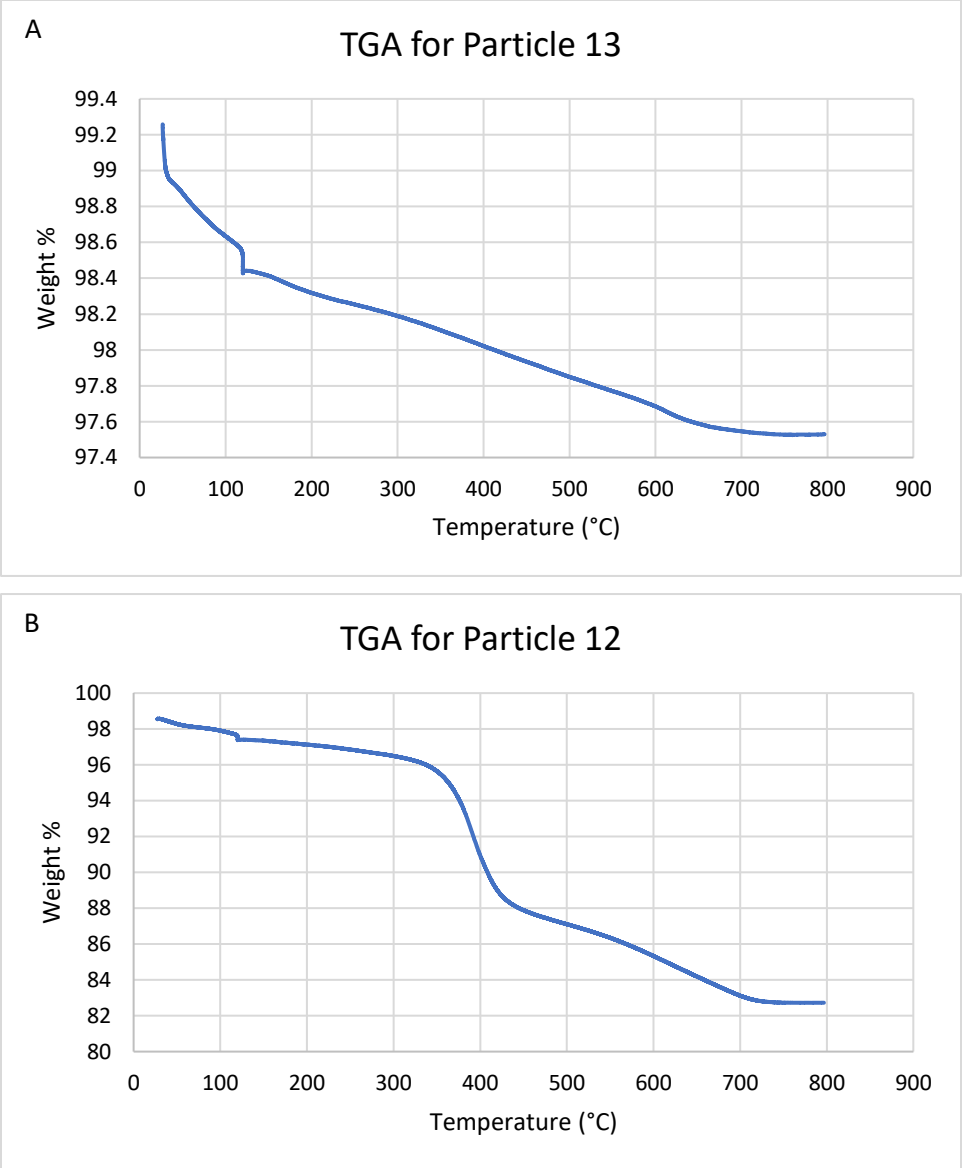

Figure 22. TGA for the S13 particles A) before PVP functionalization and B) after PVP functionalization. The particles sampled were 12 and 13 (Appendix, Table 1)

Testing the Viscoelastic Change in the System

In order to get an idea of how fast the hydrates built up in our system, it was put in a temperature-controlled rheometer. Due to limitations in availability, the geometries available to test our samples were a concentric cylinder and a vane geometry. The issue we found here was that neither were able to get a viscoelastic measurement for our system. The curves would rise slightly and then show a gradual decrease in viscosity over

time for the system utilizing the van geometry (figure 23). The obtained using the concentric cylinder showed similar results. The inability to measure a viscoelastic increase is likely due to the sedimentation of hydrates in the system. The best solution in the future for this would be to try to modify the density of the system or change the geometry to the helical one commonly used with hydrate systems to stir up the system. More testing will need to be done for the rheology of this system, but there was most certainly hydrate formation visible in the rheometer.

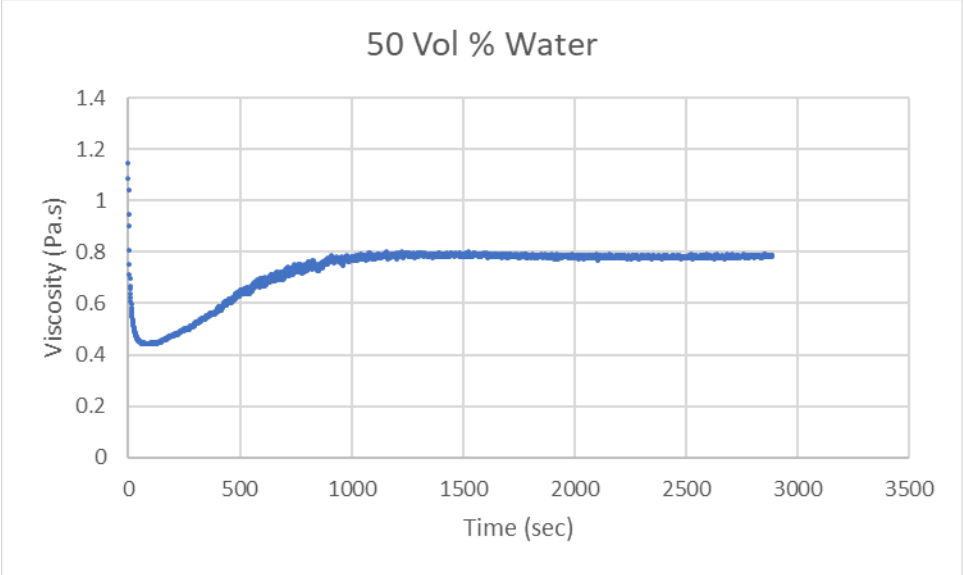

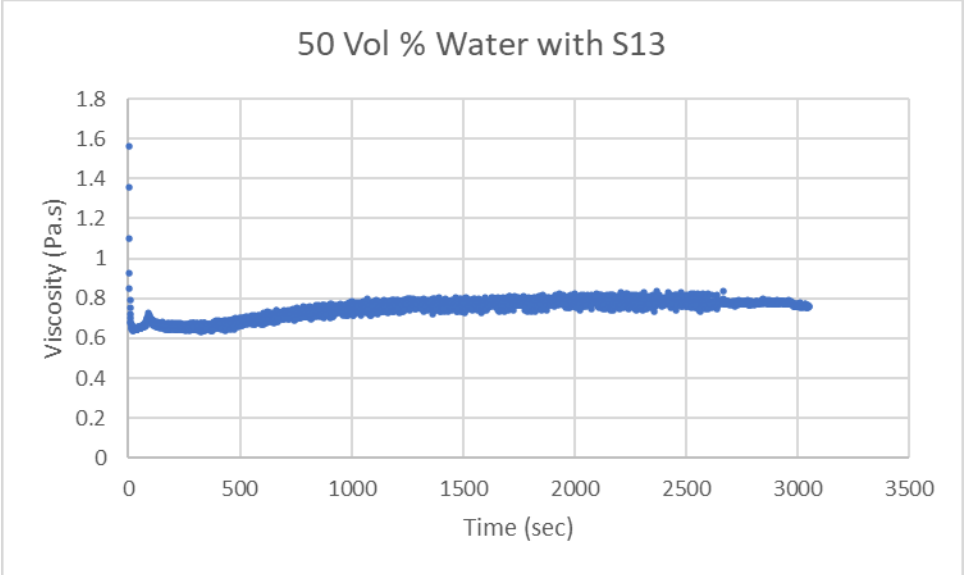

Figure 23. Viscoelastic change over time for hydrate formation in a particle and particle free system using a vane geometry. The systems were a 50-50 volume mixture of water and cyclopentane. One sample had particles dispersed in the water and the other was a control with none. The little to no change in viscosity indicates that the viscoelastic change was not recorded by the rheometer despite the formation of hydrates occurring, likely due to sedimentation in the system.

Chapter 4: Conclusion and Future Directions

This work aimed to find a method of hydrate inhibition that covered the flaws of solid particles and kinetic inhibitors by combining them. It can be concluded from the experiments done that the inhibitor we made did in fact have an effect on the hydrate formation in the system, however no trend could be found to correlate the concentration of particles to the hydrate end time of formation. It does appear that the inhibitor is negating the formation of hydrates to a degree, but it is hard to say how the inhibitor would work in a moving system under stress and pressure. Particles themselves show promise and can potentially become better hydrate inhibitors with the right combination of kinetic inhibitor. Current attempts have not yielded a consistent method of hydrate inhibition, but has shown that it is possible to inhibit hydrate formation using this method.

While these attempts did not yield a concrete inhibitor, there is still more testing that can be done before this type of inhibitor is ruled out completely. There are many different particle systems being tested as hydrate inhibitors and the method of combining two inhibitors could be promising in the future. More testing is important, even for these systems as the parameters they were tested under only yielded qualitative data. A proper rheological analysis will provide insight into the AA effect of the inhibitor which wouldn't be seen by the microscope system. DSC analysis would give a better picture of the hydrate induction and end time of formation, which is important when looking at such volatile systems. Hydrate inhibition has been studied for decades and there is still much improvement that can be made in the field.

References

(1) Fink, J. Gas Hydrate Inhibition. *Guid. to Pract. Use Chem. Refineries Pipelines* **2016**, 37–55. https://doi.org/10.1016/b978-0-12-805412-3.00004-0.

(2) Cheng, C.; Wang, F.; Tian, Y.; Wu, X.; Zheng, J.; Zhang, J.; Li, L.; Yang, P.; Zhao, J. Review and Prospects of Hydrate Cold Storage Technology. *Renew. Sustain. Energy Rev.* **2020**, *117* (December 2018), 109492. https://doi.org/10.1016/j.rser.2019.109492.

(3) Sum, A. K.; Koh, C. A.; Sloan, E. D. Clathrate Hydrates: From Laboratory Science to Engineering Practice. *Ind. Eng. Chem. Res.* **2009**, *48* (16), 7457–7465. https://doi.org/10.1021/ie900679m.

(4) Subramanian, S.; Kini, R. A.; Dec, S. F.; Sloan, E. D. Evidence of Structure II Hydrate Formation from Methane + Ethane Mixtures. *Chem. Eng. Sci.* **2000**, *55* (11), 1981–1999. https://doi.org/10.1016/S0009-2509(99)00389-9.

(5) Yegya Raman, A. K.; Koteeswaran, S.; Venkataramani, D.; Clark, P.; Bhagwat, S.; Aichele, C. P. A Comparison of the Rheological Behavior of Hydrate Forming Emulsions Stabilized Using Either Solid Particles or a Surfactant. *Fuel* **2016**, *179*, 141–149. https://doi.org/10.1016/j.fuel.2016.03.049.

(6) Ahuja, A.; Iqbal, A.; Iqbal, M.; Lee, J. W.; Morris, J. F. Rheology of Hydrate-Forming Emulsions Stabilized by Surfactant and Hydrophobic Silica Nanoparticles. *Energy and Fuels* **2018**, *32* (5), 5877–5884. https://doi.org/10.1021/acs.energyfuels.8b00795.

(7) Kroelein, K. G.; Muzny, C. D.; Kazakov, A. F.; Diky, V.; Chirico, R. D.; Sloan, E. D.; Frenkel, M. D. No Title https://www.nist.gov/publications/clathrate-hydrate-physical-property-database.

(8) Kirchner, M. T.; Boese, R.; Billups, W. E.; Norman, L. R. Gas Hydrate Single-Crystal Structure Analyses. *J. Am. Chem. Soc.* **2004**, *126* (30), 9407–9412.

https://doi.org/10.1021/ja049247c.

(9) Christiansen, R. L.; Sloan, E. D. Mechanisms and Kinetics of Hydrate Formation. *Ann. N. Y. Acad. Sci.* **1994**, *715* (1), 283–305. https://doi.org/10.1111/j.1749-6632.1994.tb38841.x.

(10) Okereke, N. U.; Edet, P. E.; Baba, Y. D.; Izuwa, N. C.; Kanshio, S.; Nwogu, N.; Afolabi, F. A.; Nwanwe, O. An Assessment of Hydrates Inhibition in Deepwater Production Systems Using Low-Dosage Hydrate Inhibitor and Monoethylene Glycol. *J. Pet. Explor. Prod. Technol.* **2020**, *10* (3), 1169–1182. https://doi.org/10.1007/s13202-019-00812-4.

(11) Reeburgh, W. S. Oceanic Methane Biogeochemistry. *Chem. Rev.* **2007**, *107* (2), 486–513. https://doi.org/10.1021/cr050362v.

(12) Dincer, I. Renewable Energy and Sustainable Development: A Crucial Review. *Renew. Sustain. energy Rev.* **2000**, *4* (2), 157–175. https://doi.org/10.1016/S1364-0321(99)00011-8.

(13) Tvaronavičienė, M.; Baublys, J.; Raudeliūnienė, J.; Jatautaitė, D. *Global Energy Consumption Peculiarities and Energy Sources: Role of Renewables*; 2019. https://doi.org/10.1016/B978-0-12-817688-7.00001-X.

(14) Mohamed, N.; Jawhar, I.; Al-Jaroodi, J.; Zhang, L. Sensor Network Architectures for Monitoring Underwater Pipelines. *Sensors* **2011**, *11* (11), 10738–10764. https://doi.org/10.3390/s111110738.

(15) Manning, F. S., R. E. T. *Oilfield Processing*; PennWell Corp, 1995.

(16) Umar, A. A.; Saaid, I. B. M.; Sulaimon, A. A.; Pilus, R. B. M. A Review of Petroleum Emulsions and Recent Progress on Water-in-Crude Oil Emulsions Stabilized by Natural Surfactants and Solids. *J. Pet. Sci. Eng.* **2018**, *165* (March), 673–690. https://doi.org/10.1016/j.petrol.2018.03.014.

(17) Taylor, C. J.; Miller, K. T.; Koh, C. A.; Sloan, E. D. Macroscopic Investigation of

Hydrate Film Growth at the Hydrocarbon/Water Interface. *Chem. Eng. Sci.* **2007**, *62* (23), 6524–6533. https://doi.org/10.1016/j.ces.2007.07.038.

(18) Makogon, Y. F. Formation of Hydrates in Shut-down Pipelines in Offshore Conditions. *Proc. Annu. Offshore Technol. Conf.* **1996**, *4* (2), 749–756. https://doi.org/10.4043/8235-ms.

(19) Akhfash, M.; Aman, Z. M.; Ahn, S. Y.; Johns, M. L.; May, E. F. Gas Hydrate Plug Formation in Partially-Dispersed Water-Oil Systems. *Chem. Eng. Sci.* **2016**, *140*, 337–347. https://doi.org/10.1016/j.ces.2015.09.032.

(20) Zhang, D.; Huang, Q.; Zheng, H.; Wang, W.; Cheng, X.; Li, R.; Li, W. Effect of Wax Crystals on Nucleation during Gas Hydrate Formation. *Energy and Fuels* **2019**, *33* (6), 5081–5090. https://doi.org/10.1021/acs.energyfuels.9b00815.

(21) Butt, H.-J.; Graf, K.; Kappl, M. *Surfactants, Micelles, Emulsions, and Foams*; 2004. https://doi.org/10.1002/3527602313.ch12.

(22) Gonzalez Ortiz, D.; Pochat-Bohatier, C.; Cambedouzou, J.; Bechelany, M.; Miele, P. Current Trends in Pickering Emulsions: Particle Morphology and Applications. *Engineering* **2020**, *6* (4), 468–482. https://doi.org/10.1016/j.eng.2019.08.017.

(23) Binks, B. P.; Lumsdon, S. O. Stability of Oil-in-Water Emulsions Stabilised by Silica Particles. *Phys. Chem. Chem. Phys.* **1999**, *1* (12), 3007–3016. https://doi.org/10.1039/a902209k.

(24) Low, L. E.; Siva, S. P.; Ho, Y. K.; Chan, E. S.; Tey, B. T. Recent Advances of Characterization Techniques for the Formation, Physical Properties and Stability of Pickering Emulsion. *Adv. Colloid Interface Sci.* **2020**, *277*, 102117. https://doi.org/10.1016/j.cis.2020.102117.

(25) Binks, B. P.; Lumsdon, S. O. Influence of Particle Wettability on the Type and Stability of Surfactant-Free Emulsions. *Langmuir* **2000**, *16* (23), 8622–8631. https://doi.org/10.1021/la000189s.

(26) Ballard, N.; Law, A. D.; Bon, S. A. F. Colloidal Particles at Fluid Interfaces: Behaviour of Isolated Particles. *Soft Matter* **2019**, *15* (6), 1186–1199. https://doi.org/10.1039/c8sm02048e.

(27) Ruckenstein, E. Microemulsions, Macroemulsions, and the Bancroft Rule. *Langmuir* **1996**, *12* (26), 6351–6353. https://doi.org/10.1021/la960849m.

(28) Zhuravlev, L. T. The Surface Chemistry of Amorphous Silica. Zhuravlev Model. *Colloids Surfaces A Physicochem. Eng. Asp.* **2000**, *173* (1–3), 1–38. https://doi.org/10.1016/S0927-7757(00)00556-2.

(29) Cha, M.; Shin, K.; Kim, J.; Chang, D.; Seo, Y.; Lee, H.; Kang, S. P. Thermodynamic and Kinetic Hydrate Inhibition Performance of Aqueous Ethylene Glycol Solutions for Natural Gas. *Chem. Eng. Sci.* **2013**, *99*, 184–190. https://doi.org/10.1016/j.ces.2013.05.060.

(30) Yagasaki, T.; Matsumoto, M.; Tanaka, H. Adsorption of Kinetic Hydrate Inhibitors on Growing Surfaces: A Molecular Dynamics Study. *J. Phys. Chem. B* **2018**, *122* (13), 3396–3406. https://doi.org/10.1021/acs.jpcb.7b10356.

(31) Palermo, T.; Sloan, D. *Artificial and Natural Inhibition of Hydrates*; Elsevier Inc., 2011. https://doi.org/10.1016/B978-1-85617-945-4.00005-4.

(32) Bavoh, C. B.; Khan, M. S.; Ting, V. J.; Lal, B.; Ofei, T. N.; Ben-Awuah, J.; Ayoub, M.; Shariff, A. B. M. The Effect of Acidic Gases and Thermodynamic Inhibitors on the Hydrates Phase Boundary of Synthetic Malaysia Natural Gas. *IOP Conf. Ser. Mater. Sci. Eng.* **2018**, *458* (1). https://doi.org/10.1088/1757-899X/458/1/012016.

(33) Kelland, M. A. History of the Development of Low Dosage Hydrate Inhibitors. *Energy and Fuels* **2006**, *20* (3), 825–847. https://doi.org/10.1021/ef050427x.

(34) Mehta, A. P.; Hebert, P. B.; Cadena, E. R.; Weatherman, J. P. Fulfilling the Promise of Low Dosage Hydrate Inhibitors: Journey from Academic Curiosity to Successful Field Implementation. *Proc. Annu. Offshore Technol. Conf.* **2002**, No. February,

565–571. https://doi.org/10.4043/14057-ms.

(35) Perrin, A.; Musa, O. M.; Steed, J. W. The Chemistry of Low Dosage Clathrate Hydrate Inhibitors. *Chem. Soc. Rev.* **2013**, *42* (5), 1996–2015. https://doi.org/10.1039/c2cs35340g.

(36) Frostman, L. M.; Przybylinski, J. L. Successful Applications of Anti-Agglomerant Hydrate Inhibitors. *SPE Repr. Ser.* **2004**, No. 58, 193–202. https://doi.org/10.2523/65007-ms.

(37) Bui, T.; Phan, A.; Monteiro, D.; Lan, Q.; Ceglio, M.; Acosta, E.; Krishnamurthy, P.; Striolo, A. Evidence of Structure-Performance Relation for Surfactants Used as Antiagglomerants for Hydrate Management. *Langmuir* **2017**, *33* (9), 2263–2274. https://doi.org/10.1021/acs.langmuir.6b04334.

(38) Lechuga, M.; Fernández-Serrano, M.; Jurado, E.; Núñez-Olea, J.; Ríos, F. Acute Toxicity of Anionic and Non-Ionic Surfactants to Aquatic Organisms. *Ecotoxicol. Environ. Saf.* **2016**, *125*, 1–8. https://doi.org/10.1016/j.ecoenv.2015.11.027.

(39) Li, H.; Stanwix, P.; Aman, Z.; Johns, M.; May, E.; Wang, L. Raman Spectroscopic Studies of Clathrate Hydrate Formation in the Presence of Hydrophobized Particles. *J. Phys. Chem. A* **2016**, *120* (3), 417–424. https://doi.org/10.1021/acs.jpca.5b11247.

(40) Yegya Raman, A. K.; Aichele, C. P. Effect of Particle Hydrophobicity on Hydrate Formation in Water-in-Oil Emulsions in the Presence of Wax. *Energy and Fuels* **2017**, *31* (5), 4817–4825. https://doi.org/10.1021/acs.energyfuels.7b00092.

(41) Tamami, B.; Allahyari, H.; Ghasemi, S.; Farjadian, F. Palladium Nanoparticles Supported on Poly (N-Vinylpyrrolidone)-Grafted Silica as New Recyclable Catalyst for Heck Cross-Coupling Reactions. *J. Organomet. Chem.* **2011**, *696* (2), 594–599. https://doi.org/10.1016/j.jorganchem.2010.09.028.

Appendix

Hydrate Formation Time Data

Table 1. List of the particle functionalizations tested including the silane(s) used, the amount of silane respectively, the functionalization solvent, and the time of functionalization. The procedure for functionalization can be found in the particle functionalization section of the experimental.

Particle	Silane	Amount	Solvent	Time	PVP
1	hexadecyl	50 µL	acetone	24 hr	no
2	hexadecyl	100 µL	acetone	1 hr	no
3	hexadecyl, vinyl	100 µL, 500 µL	acetone	24 hr	yes
4	hexadecyl	100 µL	acetone	24 hr	no
5	hexadecyl	150 µL	acetone	1 hr	no
6	hexadecyl	150 µL	acetone	24 hr	no
7	hexadecyl	200 µL	acetone	1 hr	no
8	hexadecyl	200 µL	acetone	24 hr	no
9	hexadecyl	250 µL	acetone	1 hr	no
10	hexadecyl	250 µL	acetone	24 hr	no
11	hexadecyl	250 µL	hexanes	24 hr	no
12	hexadecyl, vinyl	500 µL, 500 µL	hexanes	24 hr	yes
13	hexadecyl	500 µL	hexanes	24 hr	no
14	hexadecyl, vinyl	750 µL, 500 µL	hexanes	24 hr	yes
15	hexadecyl	750 µL	hexanes	24 hr	no
16	hexadecyl, vinyl	1 mL, 500 µL	hexanes	24 hr	yes
17	hexadecyl	1 mL	hexanes	24 hr	no
18	octyl	50 µL	acetone	24 hr	no
19	octyl	100 µL	acetone	1 hr	no
20	octyl	100 µL	acetone	24 hr	no
21	octyl	150 µL	acetone	1 hr	no
22	octyl	150 µL	acetone	24 hr	no
23	octyl	200 µL	acetone	1 hr	no
24	octyl	200 µL	acetone	24 hr	no
25	octyl	250 µL	acetone	1 hr	no
26	octyl	250 µL	acetone	24 hr	no
27	octyl	400 µL	acetone	24 hr	no
28	octyl	750 µL	acetone	24 hr	no
29	octyl	1 mL	acetone	24 hr	no
30	octyl	1.25 mL	acetone	24 hr	no
31	vinyl	100 µL	acetone	24 hr	yes
32	vinyl	100 µL	acetone	24 hr	no
33	vinyl	500 µL	acetone	24 hr	yes
34	vinyl	500 µL	acetone	24 hr	no
35	vinyl	1 mL	acetone	24 hr	yes
36	vinyl	1 mL	acetone	24 hr	no

Table 2. Data for the hydrate induction and end time of formation for a surfactant only system (figure 13).

	Induction Time (min)	End of Hydrate Formation (min)	Stdev induction	Stdev end
1 wt % Span 65	7.8	57.7	2.4	2.1
0.25 wt % Span 65	9.3	74.0	3.0	26.6

Table 3. Data for the average hydrate induction and end time of formation for hydrate systems with both particles and surfactants (figure 14).

	Induction Time (min)	End of Hydrate Formation (min)	Stdev induction	Stdev end
0.1 wt %	4.8	49.8	1.0	17.6
0.25 wt %	6.2	59.3	0.6	1.2
1 wt %	5.7	56.5	2.3	3.0
2 wt %	5.5	56.7	0.9	4.2
4 wt %	5.0	110.0		
6 wt %	13.5	65.0		
10 wt %	4.5	120.0		

Table 4. Data for the hydrate induction and end time of formation for the silane particle controls (figure 18).

	Induction Time (min)	End of Hydrate Formation (min)	Stdev for induction	Stdev for end
10 wt % Particle 32	6.3	65.0	2.0	8.7
6 wt % Particle 32	5.0	75.0		
4 wt % Particle 32	6.0	70.0		
1 wt % Particle 32	12.0	120.0		
0.1 wt % Particle 32	10.0	90.0		
0.1 wt % Particle 34	5.0	88.0		
1 wt % Particle 34	2.0	75.0		
4 wt % Particle 34	6.8	95.0	1.8	7.1
6 wt % Particle 34	5.0	65.0		
10 wt % Particle 34	5.5	75.0	2.1	21.2
0.1 wt % Particle 36	6.0	70.0		
1 wt % Particle 36	2.5	50.0		
2 wt % Particle 36	4.5	47.0		
4 wt % Particle 36	5.0	77.5	0.7	3.5
5 wt % Particle 36	5.0	70.0		
6 wt % Particle 36	5.0	65.0		
10 wt % Particle 36	8.0	75.0	1.4	7.1

Table 5. Data for the average induction and end time of formation for the PVP only hydrate formation system (figure 19).

	Induction Time (min)	End of Hydrate Formation (min)	Stdev for induction	Stdev for end
1 wt % PVP	9.0	70.3	2.3	8.2
0.1 wt % PVP	8.8	76.0	4.3	8.5
0.01 wt % PVP	4.5	84.3	0.5	30.9

Table 6. Data for the induction and end time of formation for the PVP and silane functionalized particles. The "+" represents hydrate formation going over the maximum recording time (figure 20).

	Induction Time (min)	End of Hydrate Formation (min)		stdev induction	stdev end
0.1 wt % Particle 31	7.0	90.0			
1 wt % Particle 31	8.7	51.0		1.4	
4 wt % Particle 31	10.3	180.0	+	1.2	
10 wt % Particle 31	10.0	120.0			
0.1 wt % Particle 33	6.5	65.0			
1 wt % Particle 33	7.3	60.0		1.2	
2 wt % Particle 33	4.5	90.0			
4 wt % Particle 33	12.5	180.0	+	3.5	
6 wt % Particle 33	6.0	60.0			
10 wt % Particle 33	11.0	140.0			
0.1 wt % Particle 35	10.0	135.0			
1 wt % Particle 35	5.8	120.0		2.5	10.0
4 wt % Particle 35	9.5	90.0			
6 wt % Particle 35	11.0	95.0			

Table 7. Data for the end time of formation (min) for the blind trials using particles 31 and 35 as the hydrate inhibitors in blind trials (figure 21).

	Normal End of Formation (min)	Blind End of Formation (min)
0.1 wt % Particle 31	127	90
1 wt % Particle 31	75	51
4 wt % Particle 31	60	180
10 wt % Particle 31	125	120
	Normal End of Formation (min)	Blind End of Formation (min)
0.1 wt % Particle 35	57	65
1 wt % Particle 35	45	60
4 wt % Particle 35	90	180
6 wt % Particle 35	115	60